Available online at BCREC website: https://bcrec.id

Bulletin of Chemical Reaction Engineering & Catalysis, 18 (4) 2023, 559-581

Review Article

SO_2 Mitigation via Catalytic Oxidation using Carbonaceous Materials and Metal Oxides for Environmental Sustainability

Tanoko Matthew Edward[1], Ying Weng[1], Sin Yuan Lai[1,2,*]

[1]School of Energy and Chemical Engineering, Xiamen University Malaysia, Jalan Sunsuria, Bandar Sunsuria, 43900 Sepang, Selangor Darul Ehsan, Malaysia.
[2]College of Chemistry and Chemical Engineering, Xiamen University, 361005 Xiamen, China.

Received: 4th September 2023; Revised: 12nd October 2023; Accepted: 13rd October 2023
Available online: 16th October 2023; Published regularly: December 2023

Abstract

The high concentration of sulfur dioxide (SO_2) in the air that contributes to increasing health and environmental issues has caught the attention of all countries. Numerous tactics to regulate and lower the SO_2 levels in the environment that have been applied through regulations and promising technology, progress has been obtained to decrease the SO_2 concentration. Among methods for SO_2 removal, one of the promising techniques used is the catalytic oxidation of SO_2 to SO_3, which not only reduces the SO_2 concentration in the environment but also produces sulfuric acid (H_2SO_4). Thus, the performance of the catalysts that can promote the catalytic oxidation of SO_2 to SO_3 for environmental sustainability is reviewed in this study. The types of catalysts evaluated in this study are carbon-based materials and metal oxides. Worth noting that these catalysts are feasible to catalytically converting SO_2 hazardous material to resources, viz. SO_3 and H_2SO_4 for industrial use. The findings of this study can serve as a foundation for devising an innovative method for SO_2 mitigation through catalytic oxidation.

Keywords: SO_2 mitigation; catalytic oxidation; carbonaceous materials; metal oxides; environmental sustainability

How to Cite: T. M. Edward, Y. Weng, S. Y. Lai (2023). SO_2 Mitigation via Catalytic Oxidation using Carbonaceous Materials and Metal Oxides for Environmental Sustainability. *Bulletin of Chemical Reaction Engineering & Catalysis*, 18(4), 559-581 (doi: 10.9767/bcrec.20031)

Permalink/DOI: https://doi.org/10.9767/bcrec.20031

1. Introduction

Until now, the world still highly depends on the fossil fuels regardless the emerging of renewable energy sources. Large-scale usage of the coal, oil, and natural gas is frequently associated with major environmental challenges, especially gaseous pollution in the atmosphere. Air quality control is one of the most pressing health and environmental issues today. This has prompted substantial research into effective technology for removing harmful gases [1–4], as well as the development of alternative clean energy sources [5–8]. Even though many wealthy countries have made significant progress in managing air pollution in recent decades; nonetheless, the approximately 28,704 kilotons of SO_2 emission in 2019 shows that the air pollution levels remain very high [9,10].

SO_2 is a prominent source of air pollution in urban areas as it is produced chiefly by the combustion of fossil fuels in vehicles, fuels of marine vessels, and industrial processing. The combustion of fossil fuels in both fixed and mobile

* Corresponding Author.
Email: sinyuan.lai@xmu.edu.my (Sin Yuan Lai)

sources emits many tons of SO_2 into the atmosphere every year. In addition to these anthropogenic sources, the natural sources, such as volcano eruption and landscape fire, also contribute to the SO_2 emission. A high amount of SO_2 emissions is correlated to a variety of health issues, including respiratory sickness and breathing difficulties, as well as environmental consequences, such as acid rain generation that is harmful to forests [11,12].

In this context, the abatement of SO_2 from the atmosphere is in accordance with UN's plan to deal with consumption and production patterns (SDG Goal 12) and life on land (SDG Goal 15). Following the United Nations Sustainable Development Goal (SDG) 12 to ensure sustainable consumption and production patterns, the target is to recover the generated pollutants, such as SO_2, from fossil fuels to valuable commodities, such as $CaSO_4$ and H_2SO_4. The reduction in SO_2 produced is in accordance with the SDG indicator 12.4 and 12.5 to manage responsibly and decrease the generation of hazardous waste [13]. On the other hand, following the UN SDG 15 to sustainably manage forests and halt biodiversity loss, the target is to reduce the occurrence of acid rain that may be harmful to the forest ecosystems. Complying to the SDG indicator 15.1 and 15.2, the removal of SO_2 produced may conserve the ecosystems and protect forests from deforestation [14].

Various strategies to control and reduce SO_2 levels in the environment have been proposed through policies or promising technologies to achieve the UN's SDGs. The National Ambient Air Quality Standard (NAAQS) has regulated the average SO_2 emission over a specified period, such as a 1-h standard for 75 ppb SO_2 concentration and a 24-h standard for 140 ppb SO_2 concentration. This aims to provide increased protection for at-risk group, such as people with asthma, and other potentially at-risk populations against a variety of adverse respiratory effects [15]. The maximum standard was derived based on the quantitative analyses regarding SO_2 exposures to people with asthma ranging from 5- to 10- minutes, whereas the standard is considered to be adequate to provide public health protection with a sufficient margin of safety. A stringent rule has been enacted by International Maritime Organization (IMO). The rule, referred to as "IMO 2020," lowers the previous limit of 3.5% to a maximum of 0.50% m/m (mass by mass) for fuel oil used on ships operating outside specified emission control areas [16]. In order to comply with the new limit, ships that typically run-on heavy oil - a higher sulphur-content byproduct of crude oil distillation - are now required to use very low sulphur fuel oil (VLSFO). This is a significant development for improving air quality, preserving the environment, and safeguarding human health [17]. In regards to one of the most contributing industries to the SO_2 emission, the petroleum industry set for the allowable sulfur content of fuel oils at 1 wt.% to limit the amount of SO_2 emission produced from the combustion equipment. Moreover, the API gravity (ratio of the mass of a given volume of oil at 60 °F to the mass of the same volume of water at 60 °F) was set to 33° API in 2035 by the World Oil Outlook [18]. Fortunately, the upcoming Industry 4.0 promotes sustainable development through the realization of the digitalization, automation, and integration in all processes. Less negative effects and more beneficial effects on the usage of resources, including materials, energy, information, and high-quality products would result from its implementation. At the early stage, the production of the infrastructure to enable the operation of Industry 4.0 is highly expensive and induce high pollution and waste in result. Nonetheless, the benefits of Industry 4.0 outweigh the drawbacks, as the efficient production process enables the reduction of energy consumed by 30% through the implementation of Internet of things (IoT) and effective use of raw materials and energy [19]. Hence, we believe that synergize Industry 4.0 and catalytic SO_2 oxidation could effectively reduce the industrial processing, energy consumption, and production costs.

The oxidation of fuel oil using hydrogen peroxide and iron oxyhydroxide, followed by extraction of oxidized sulfur compounds with aqueous acetonitrile is one of the most advanced methods of removing sulfur directly from fuel oil [20]. Another method is through reducing SO_2 production and release from flue gas, which can be resolved using many catalysts. Wu *et al.* [21] proposed the usage of $^{\bullet}OH$ from catalytic decomposition of gas-phase H_2O_2 over solid-phase $Fe_2(SO_4)_3$ which can reach 99.8% SO_2 removal at 140 °C. Oxidative absorbents like $NaClO_2$ and CaO_2 also can be used to remove SO_2 in wet conditions [22], moreover, CaO that can be obtained from coconut shell char was proved to be a good eco-friendly catalyst for SO_2 removal [23].

Among the methods devised for SO_2 removal, the catalytic oxidation of SO_2 to SO_3 is critical because it not only removes hazardous SO_2 but also provides a mechanism for producing SO_3, which is an important reaction in the industry for preparing sulfuric acid (H_2SO_4).

Thus, the removal of SO_2 from the atmosphere will not only beneficial to comply with UN's SDGs 12 and 15 but also promoting waste-to-resources action by producing useful H_2SO_4. The industrial compound, H_2SO_4, is widely in fertilizer manufacturing, particularly phosphate fertilizers made from wet-process phosphoric acid. In 2018, the global H_2SO_4 market was valued at 266.2 million tons, and it is predicted to grow at a CAGR of 2.3 percent from 2019 to 2027, and is expected to exceed 324.1 million tons by 2027 [24]. As a result, throughout the last few decades, significant research [25–29] have been devoted to developing low-cost and effective catalysts for the oxidation of SO_2 to SO_3. It should also be noted that this treatment does not entail the transfer of contaminants from one medium to another, such as from air to water. Instead of changing the pollutants' medium, SO_2 is transformed to H_2SO_4, which can be used to make beneficial fertilizers and chemicals.

The importance to find the most suitable catalyst to remove SO_2 from the air is shown through the number of researches completed relating to SO_2 oxidation. The growing trend of published research papers in the field of SO_2 oxidation is illustrated statistically in Figure 1. In the last ten years, about 4805 papers related to SO_2 oxidation have been published on Web of Science with the keyword of SO_2 oxidation. The number of publications has increased dramatically from 248 publications in 2013 to 606 publications in 2021, the number of citations also spike up to 21483 in year 2022.

Even though numerous researches have been conducted on SO_2 oxidation into SO_3, no comprehensive review has been carried out to investigate the catalytic SO_2 oxidation over carbonaceous materials and metal oxides. Herein, we conduct a systematic study to discuss these catalysts, ranging from materials engineering and structure-property relationships to catalytic efficiency. The fundamental knowledge of SO_2 catalytic oxidation is depicted with mechanistic pathways; meanwhile, the intensifying catalytic process is scrutinized with influencing factors. The findings of this study help establish an innovative path for future SO_2 removal prospects, considering the cost and effectiveness. This research could be beneficial to the human environment's cleanup and to maintain the longevity of the earth itself.

2. Fundamentals of SO_2 Catalytic Oxidation

The basic principle of SO_2 catalytic oxidation follows the elementary reaction mechanism of:

$SO_2 + ½\ O_2 \rightarrow SO_3$ (Eq. 1) ×2
$2\ SO_2 + O_2 \rightarrow 2\ SO_3$ ΔH = -197.8 kJ/mol;
ΔG = -371.7 kJ/mol

whereas, the SO_2 reacts with O_2 that acts as the oxidant to obtain SO_3 in return. Moreover, with the presence of water the SO_3 is hydrolyzed and H_2SO_4 is formed from the reaction (Eq. 2) [25]:

$SO_3 + H_2O \rightarrow H_2SO_4$ (Eq. 2)
ΔH = -227.1 kJ/mol
ΔG = -302.1 kJ/mol

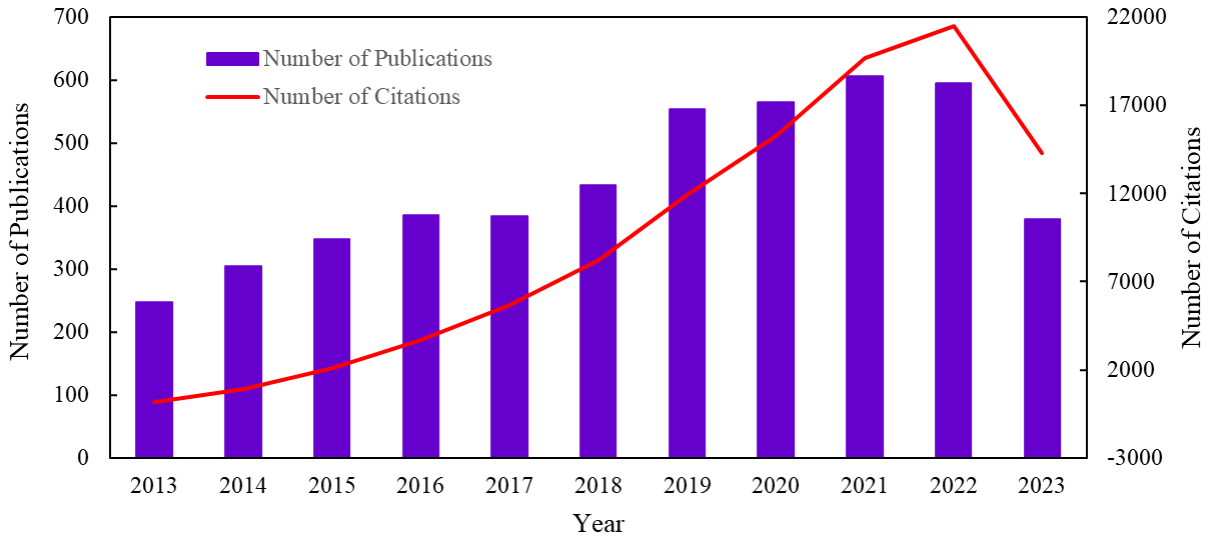

Figure 1. The number of published and cited articles related to SO2 oxidation per year from 2013 to 2023 (as of 12 October 2023, Web of Science)

Equations (1) and (2) show negative values for both standard enthalpy changes (-ΔH) and standard Gibbs free energy changes (-ΔG), indicating the reactions are exothermic, thermodynamically favorable and proceeds spontaneously in the forward direction at a given standard conditions (25 °C and 1 atm). However, the different catalysts used leads to different non-elementary reactions. The differences can be from the types of adsorptions that occur, the side or non-elementary reactions, and the intermediates.

For the carbonaceous materials catalysts (Figure 2), the SO_2 is adsorbed into the surface of the catalysts, while the O_2 may also be adsorbed (for carbon-doped boron nitride) or not (for activated carbon), following the Eley-Rideal mechanism [25,27]. Similarly, the metal oxides, such as Pt, Ag, Au, VO_x/SiO_2, MnO_x/SiO_2, and CuO_x/SiO_2, provide the required active sites for catalytic oxidation of SO_2 [31]. Note that SO_2 and O_2 are chemisorbed in several metal oxides, for example, in Pt (Figure 3) and Ag [32].

3. Types of Catalysts

3.1 Carbonaceous Materials

3.1.1. Activated carbon

Activated carbon (AC) has been identified as an effective adsorbent and catalyst to clean stack gases, especially in SO_2 removal [34]. The highly-porous structure of activated carbon supports SO_2 removal as it is effective for not only adsorbing SO_2 but also storing the H_2SO_4 produced after SO_2 oxidation. The removal of SO_2 by using activated carbon was divided into two parts. First, the SO_2 was extracted from the flue gas by adsorption into the activated carbon due to the basic surface chemistry of the highly-porous activated carbon. Then, the adsorbed SO_2 was catalytically oxidized into sulfuric acid in the presence of oxygen and water vapour, and stored in the activated carbon pores subsequently [25]. Note that the SO_2 conversion processes occur in the micropores of porous carbon materials due to their necessity for spatial confinement, specialized chemical functionalities, and sufficient specific surface areas [35].

The reaction mechanism of SO_2 removal by activated carbon with the presence of O_2 and H_2O is shown in Eqs. 1-5:

$$SO_{2(gas)} + AC \rightarrow SO_{2(ad)} \quad \text{(Eq. 3)}$$
$$H_2O_{(gas)} + AC \rightarrow H_2O_{(ad)} \quad \text{(Eq. 4)}$$
$$SO_{2(ad)} + \tfrac{1}{2}\, O_{2(gas)} \rightarrow SO_{3(ad)} \quad \text{(Eq. 1)}$$
$$SO_{3(ad)} + H_2O_{(ad)} \rightarrow H_2SO_{4(ad)} \quad \text{(Eq. 2)}$$
$$H_2SO_{4(ad)} + H_2O_{(l)} \rightarrow H_2SO_{4(l)} \quad \text{(Eq. 5)}$$

where, AC is for activated carbon, (g) is for gas phase, (ad) as the adsorption state, and (l) is for liquid phase [25]. Based on the reaction mechanism, the reaction follows the Eley-rideal mechanism, whereas a molecule (SO_2) adsorbs onto the surface (activated carbon) and another molecule (O_2) interacts with the adsorbed one until a product (SO_3) is formed and desorbs from the surface (after attaching with water).

One enhancement on the use of activated carbon in SO_2 removal is the use of a tailored activated carbon fiber (ACF) which has a specific tailored micro-mesoporous structure [36]. Diez *et al.* [36] found that with the presence of micropores and large mesopores in the Co-ACF, higher catalytic activity in the activated carbon can be achieved. The tailored Co-ACF was obtained by catalytic steam activation of the Cobalt naphthanete-doped coal-based carbon fibers, and continued with impregnation with KOH to induce basicity to the ACF sur-

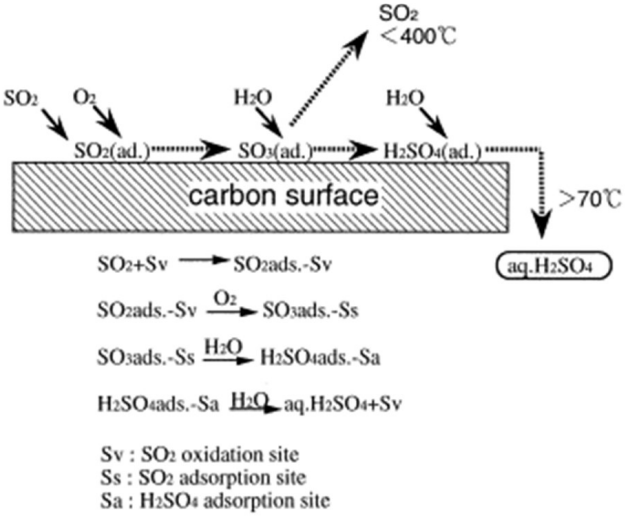

Figure 2. Mechanism of SO_2 removal using carbonaceous material catalysts [30]

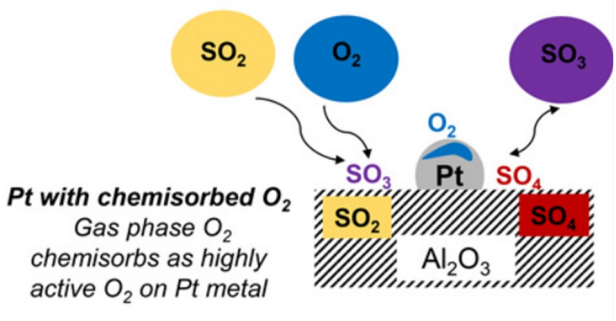

Figure 3. Mechanism of SO_2 removal using metal oxides (Pt) [33]

face that assists in the catalytic activity. The difference in the surface structure of the ACF and Co-ACF is shown in Figure 4. The activation process was done in a quartz crucible where the Co-ACF was half-burnt at 850 °C with the flow of water vapor. The half-burnt condition is crucial as the burnt area provides mesopores and the unburnt portion produces micropores. This tailored Co-ACF shows a higher catalytic activity of 105 μmol.min^{-1}. g^{-1} in 15 min, as compared to the non-doped ACF with only half of the catalytic activity in 28 min. The combination of micropores and mesopores enhances the diffusion for the adsorption and desorption of the substances involved in SO_2 removal, resulting in significantly increased oxidation rates - as the O-enriched ACF (mesopores) is comparatively active with the N-enriched ACF (micropores). Therefore, using cobalt naphthenate as cobalt nanoparticle precursor not only leads to tailored porous activated carbon with enhanced effectiveness, but also provides higher catalytic activity compared to other non-doped ACF. In addition, the use of cobalt naphthenate also covers up the low catalytic activity of activated carbon towards SO_2 removal, and caters to good absorbability of the carbon.

An alternative metal precursor, Vanadium Pentoxide (V_2O_5), could also be embedded in the ACF, as the catalyst still maintain its catalytic activity towards SO_2 oxidation after the formation of Vanadium Sulfate ($V_2O_3(SO_4)_2$) [37]. In fact, several catalysts that can be used to assist the activated carbon in removing SO_2 from flue gas, however, most of them require high temperatures to operate. At lower temperatures (100–250 °C), the active components, i.e. metal oxides, is deactivated to form metal sulfates under SO_2 that impedes the removal. Jing et al. [34] also add that V_2O_5 is promising as it shows strong SO_2 adsorption at stack temperatures (120–200 °C) and improves the reaction process with the presence of oxygen. The two steps on how the Vanadium used in the SO_2 removal process, were then expressed by Guo *et al.* [38] and can be seen in Figure 5. First, the reaction between V_2O_5 with SO_2 during oxidation formed a vanadium sulfate, $V_2O_3(SO_4)_2$, which trapped SO_2 in the catalyst. Nevertheless, unlike many metal oxides, such as CuO, Fe_2O_3, and MnOx, that deactivates in their sulfates form [38], the vanadium sulfate does not deactivate but can act as a stable active component to catalyze SO_2 oxidation into H_2SO_4 [38]. Whereas, the activity of Vanadium Sulfate is proved by the existence of characteristic bands at 1011 cm^{-1} due to ν(V=O), 535 cm^{-1} due to ν(S-O-V), and 750 cm^{-1} due to ν(V-O-V) [37]. In addition, the vanadia species is more active towards SO_2 removal due to the basicity that emerges after carbon interacts with the vanadia species and increases the electron density of the species.

Guo *et al.* [38] also emphasized the activated carbon pores that is also occupied with the vanadium sulfate would reduce the H_2SO_4 formed due to the lack of storage. An experiment conducted by Jing *et al.* [37] supports this finding shown by a decrease in BET surface area and total pore volume of the activated carbon. Therefore, the quantity of V_2O_5 needs to be maintained at below 5 wt.% to ensure a high H_2SO_4 formation instead of the vanadium sulfate in the activated carbon pores [38]. Jing *et al.* [37] further supported with the results from another experiment that Vanadium catalyst with a content of 5 wt.% shows high activity and selectivity at low temperatures that promote SO_2 removal. Thus, the amount of 5 wt.% of V_2O_5 is determined to be the effective amount for SO_2 removal, and can be used in further experiments.

The presence of O_2 and H_2O, reaction temperature, and a higher initial SO_2 concentration have a drastic effect on the adsorption of SO_2. In an experiment done by Li & Ma [25], the time to achieve saturated SO_2 adsorption increases as O_2 and H_2O are introduced to the system. They found that O_2 and H_2O promote

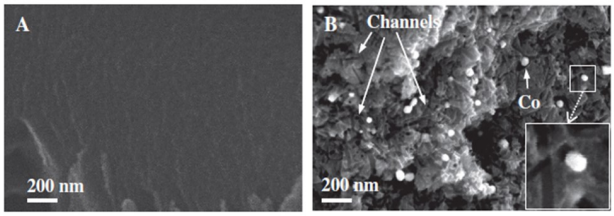

Figure 4. Surfaces of (A) ACF and (B) Co-ACF obtained from a Scanning Electron Microscopy (SEM) [36]

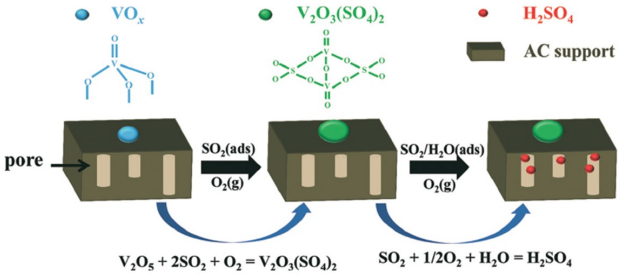

Figure 5. Schematic illustration on the mechanism of SO_2-to-H_2SO_4 over the V_2O_5/AC catalyst [38]

the removal of SO_2 by converting SO_2 into sulfuric acid. The claim that the addition of H_2O boosta the SO_2 removal is also approved by Jing *et al.* [37] that in the presence of water vapor, the peak intensity of sulfate species is 40 times more than in the absence of water when observed using IR spectra. Another experiment done by Li & Ma [25] shows that both the SO_2 adsorption rate and capacity reduce as the reaction temperature increases from 65°C. Not only does reaction temperature influence SO_2 adsorption onto activated carbon, but it also influences SO_2 catalytic oxidation into H_2SO_4. Since the adsorption process is instant and exothermic, an increase in the reaction temperature is not benefit SO_2 adsorption, as a specific temperature is required for the catalytic oxidation of SO_2. In addition, the activation energy is -16.344 kJ/mol, which indicates that the SO_2 adsorption rate decreases with increasing reaction temperature [25]. The last experiment done by Li & Ma [25] shows that an increase in the initial SO_2 concentration increases the initial SO_2 adsorption rate, as a higher initial SO_2 concentration gives more driving force for the SO_2 to be adsorbed.

3.1.2 Carbon nanotubes

Similar to activated carbon, carbon nanotubes are also porous carbon-based catalysts. One of its widely used types is the N-doped single-walled carbon nanotubes (SWCNTs) which have a low energy barrier for O_2 dissociation of 0.3 eV that causes SO_2 oxidation to be thermodynamically favorable and kinetically attainable [39]. N doping promotes catalytic desulphurization through the interaction between the lone pair electrons of nitrogen dopant and the π-bonds of carbon materials, which then affect the properties of the materials due to the difference in electronegativity. Specifically, graphite N doping can enhance the dissociation of O_2, as the reaction energies and barriers are lower than the counterparts of pyridine N doped SWCNTs [39]. Moreover, it is found that to maximize the activity for the dissociation of O_2, Gr2N-SWCNT (dual nitrogen atoms doped graphite in SWCNTs) gave a smaller diameter compared to GrN-SWCNT (singe nitrogen dopant), can be used. However, it is important to note that as a smaller diameter SWCNT is used, even though it enhances O_2 activation, a strong covalent interaction between SO_3 and the carbon nanotubes is formed; hence, impeding SO_3 desorption for catalytic loop recovery [39]. Moreover, it is found that the presence of water inhibits SO_3 desorption due to the conversion of tridentate sulfate to the more stable bidentate sulfate [40].

Other than the diameter of the pores, the curvature of the pores is also found to affect SO_2 oxidation. With the increase of the curvature (Figure 6), the adsorption energy on SO_2 increases in a negative value, indicating an exothermic process that is thermodynamically favored. According to the population analysis using the Bader method, there is a monotonic increase of electron transfer to the adsorbed SO_2 or SO_3 molecule as the curvature increases, indicating stronger electrostatic interaction for adsorption. Moreover, the SO_2 oxidation using SWCNT is found to have a positive energy barrier and negative reaction energy (exothermic reaction). By increasing the curvature, the energy barrier decreases, and the oxidation reaction energy increases in a negative value. The increase in oxidation activity due to increased curvature is proved through the increase in energy at maximum projected density of states (PDOS) in the highest occupied molecular orbital (HOMO) for both the circumferential (from −3.02 eV to −2.18 eV) and axial (from −2.40 eV to −2.18 eV) case. Moreover, in regards to the energy barrier, increasing SWCNT curvature promotes electron transfer to achieve charge compensation that results in a reduced energy barrier [41].

Another type of carbon nanotubes is the multi-walled carbon nanotubes (MWCNTs). Red mud (RM) is a solid waste produced in the process of extracting alumina and combined with the MWCNT to produce hybrid RM-CNTs. The use of this hybrid material is to further reduce waste and look at how RM as an adsorbent could activate H_2O_2 for SO_2 removal. The removal process is based on a dual-loop desul-

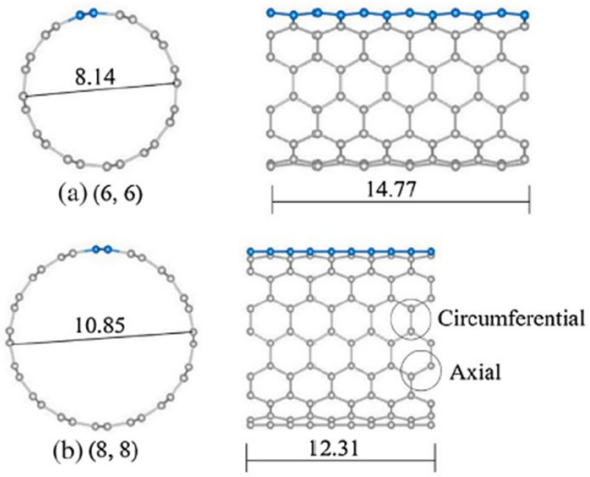

Figure 6. Structures of (6,6)- and (8,8)-SWCNTs [41]

furization absorption system in which primary-absorber is used to scrub SO_2 by RM slurry, then the SO_2 residual can be oxidized by the vaporized H_2O_2/catalysts in the catalytic system (Figure 7) [42]. Note that the multi-walled carbon nanotubes made by red mud did not show a higher efficiency than SWCNTs; however, it provides a low-cost and environmentally friendly route in producing the catalysts, which reduces the disposal of waste-solid. Moreover, the modification of the carbon nanotubes by using phosphoric acid could retain the FeOx as much as possible, increasing the active sites and the overall removal efficiency by 6% [42].

3.1.3 Graphene oxide

Graphene is also a widely known 2D carbon nanomaterial to be used in SO_2 removal at low temperatures (150 °C) [43]. The benefit of using graphene is its convenience in grafting hydroxyl and epoxy groups on its surface to produce graphene oxides (GO). The hydroxyl group in the surfaces of these graphene oxides induces a strong hydrogen-bonding interaction with SO_2 - SO_2 is a polar molecule. Moreover, there is also van der Waals intermolecular forces between the electrophilic SO_2 (and SO_3) molecules and the metallic graphene-like surface that increases SO_2 adsorption into the graphene oxides. Regarding SO_2 removal, the several kinds of graphene oxides formed after the grafting have different oxidation degrees following GP < HO_GP < O_GP < HO_OGP, with HO_OGP having the highest oxidation degree. The increasing adsorption energy follows a similar trend as in the oxidation degrees with SO_2/GP (−0.25 eV) < SO_2/O_GP (−0.30 eV) < SO_2/HO_GP (−0.38 eV) < SO_2/HO_OGP (−0.40 eV), except for the introduction of OH group, that increases the adsorption energy of SO_2/HO_GP, even though the oxidation degree of SO_2/O_GP is higher. Moreover, the oxidation barrier for SO_2 on HO_GP is 0.12 eV which is lower as compared to SO_2 on O_GP with 0.21 eV, thus implying that the hydroxyl group promotes SO_2 oxidation kinetically (Figures 8 and 9). The lower oxidation barrier is achieved as the transition state is achieved faster on HO_OGP leading to a reduced oxidation barrier compared to O_GP [44]. Overall, the addition of hydroxyl groups on the surface of graphene oxides acts as an SO_2 hunter to enhance adsorption and an epoxy activator to decrease the oxidation barrier [44]. Moreover, in terms of SO_2 oxidation by O_2, it is found that the O_2 dissociation energy barrier is reduced from 1.53 to 1.25 eV with the presence of hydroxyl groups nearby, hence promoting O_2 activation [45].

Another research was performed to further understand the role of the hydroxyl group in SO_2 removal by the addition of a second hydroxyl group into the graphene oxide, forming 2HO_OGP. The addition of a new hydroxyl group increases the adsorption energy of SO_2/2HO_OGP is increased to -0.58 eV, while the oxidation barrier is reduced to 0.06 eV, both promoting the SO_2 removal. Two hydro-

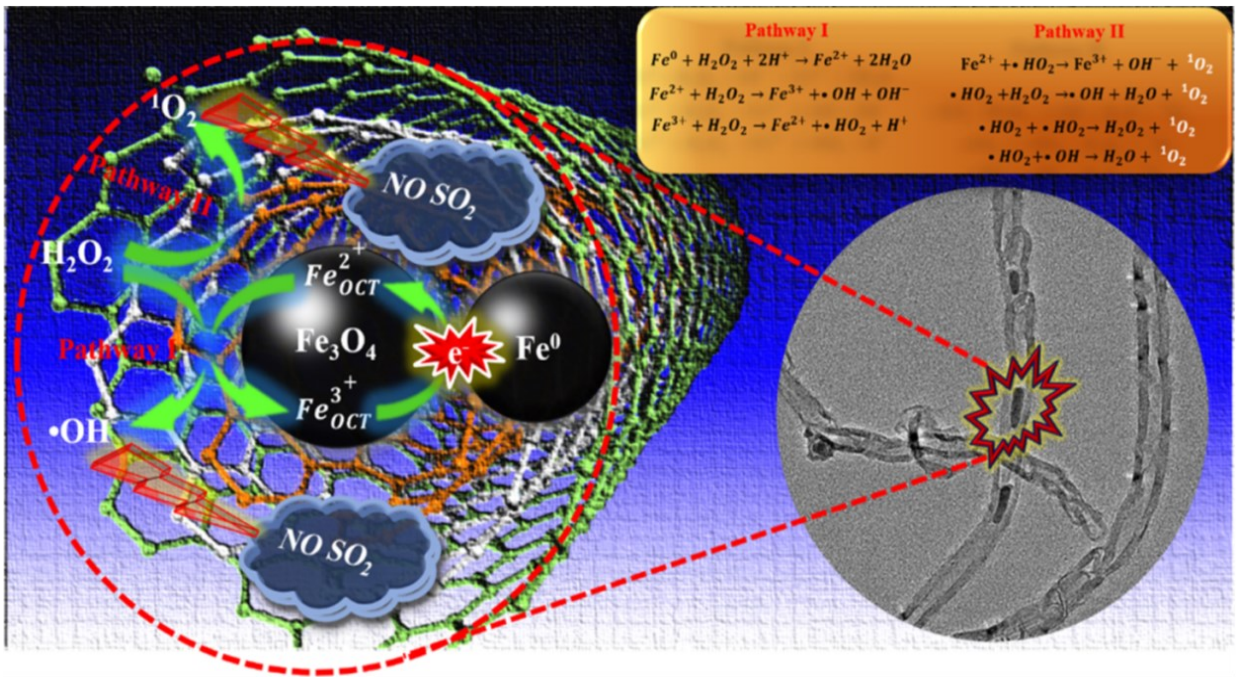

Figure 7. Mechanism of SO_2 removal by MWCNT [42]

gen bonds are formed between each of the two hydroxyl groups and the two oxygen atoms of the adsorbed SO_2 molecule, forming charge transfer channels to transfer electrons from the hydroxyl group into the SO_2, and in turn to the epoxy group. Wherein, the charge transfer will promote the pre–activation of the epoxy group in the initial adsorption configuration for further oxidation. Furthermore, the epoxy group also receives a substantial charge from SO_2 during the reaching of the transition state, which helps reducing the oxidation barrier. It is thus can be affirmed that the introduction of more hydroxyl groups enhances the adsorption and oxidation of SO_2 as more charge transfer channels are formed [43]. The reaction mechanism is shown in Eqs. 6-7 and Figure 10:

$SO_2 + 2HO\_OGP \rightarrow SO_2/2HO\_OGP$ (Eq. 6)
$SO_2/2HO\_OGP \rightarrow SO_3/2HO\_GP$ (Eq. 7)

The effect of water in the early stages of SO_2 removal using graphene oxides is also found to be very crucial, as H_2O is not only used in the hydration of SO_3 to form H_2SO_4. In the early stages of SO_2 removal, water molecules are dissociated into hydroxyl groups that promote SO_2 removal, by enhancing the O_2 dissociation and stimulating SO_2 oxidation. Even though the reaction of splitting water into hydroxyl groups is endothermic (0.44 eV) with a high energy barrier (0.90 eV), but with the existence of two hydroxyl groups near the water (in graphene oxides surface), a lower energy barrier (0.50 eV) can be achieved [45]. Another research also found that the SO_2 can be hydrated to form bisulfite, which is readily oxidized to form H_2SO_4; hence, proposing another pathway of SO_2 catalytic oxidation. The addition of water may also make the transition state of SO_2 oxidation stable due to the asymmetric spin density out of the plane, which decreases the energy barrier and increases reaction energy. Moreover, the hydroxyls that were formed from H_2O dissociation can be recovered and used in another reaction [46].

3.1.4 Carbon-doped boron nitride

Akin to graphene oxide (GO) that has a single layer of carbon atoms, carbon-doped hexagonal-boron nitride nanosheets (h-BNNS) recently also received quite an attention for their oxidation ability in SO_2 removal. Their alternating boron and nitrogen atoms give them a high thermal and mechanical stability, which will provide the required electrical and chemical properties for SO_2 removal. Moreover, the presence of partially ionic B-N bonds makes h-BNNS have higher thermal stability as compared to graphene. The introduction of carbon into h-BNNS can alter the electron density distribution of h-BNNS, which forms a new localized state above the Fermi level, resulting in a decrease in the band gap of the pristine h-BNNS. Thus, it can be concluded that the C-doping enhances the surface reactivity of h-BNNS required for SO_2 removal through the charge-transfer effects [47]. Moreover, two types of C-embedded h-BNNSs that can be produced, C_B and C_N, in which a boron and a nitrogen atom of BN sheet is substituted with a C atom, respectively (Figure 11). The C atom, which is present in both C_B and C_N, is situated on the vacancy site and creates three chemical interactions with nearby boron or nitrogen atoms. The introduction of a carbon atom alters

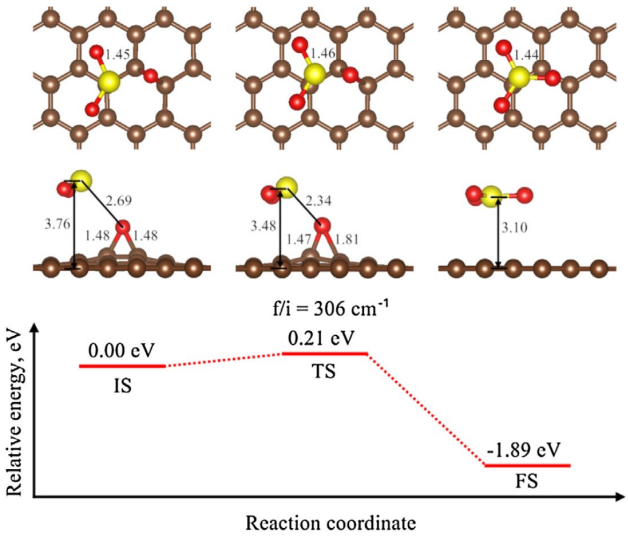

Figure 8. Oxidation of SO_2 with graphene oxide on O_GP [44]

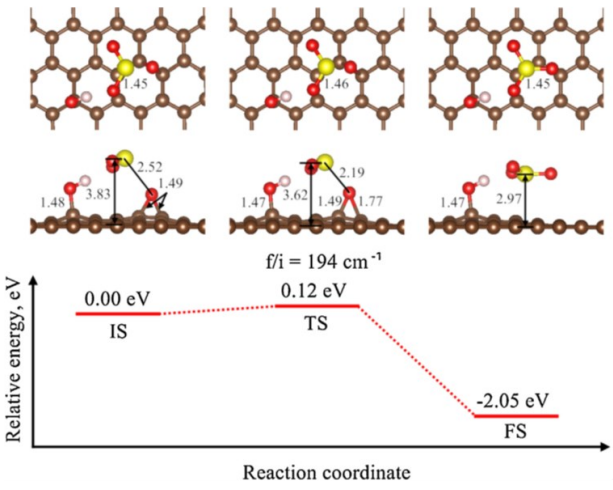

Figure 9. Oxidation of SO_2 with graphene oxide on HO_OGP [44]

the electron distribution of h-BNNS. Due to the C atom has one less valence electron than N, the C atom in C_B possesses an electron acceptor property when surrounded by N. On the other hand, the C atom has one more valence electron than B, which grants the electron donor property to the C atom in C_N when surrounded by B [47].

In regards to the SO_2 oxidation, the process starts from the co-adsorption of SO_2 and O_2 molecules to the surface of C-doped h-BNNS. Next, one oxygen atom in the adsorbed O_2 approaches the S atom of SO_2 to reach the transition state and forms SO_3. In contrast to the Eley-Rideal mechanism that occurs when activated carbon is used, by using the C-doped Boron nitride, the reaction follows the Langmuir-Hinshelwood mechanism. The mechanism happens when two molecules (SO_2 and O_2) adsorb onto the surface and diffuse and interact with each other until a product is formed and desorbs from the surface. However, SO_2 oxidation can only occur on the boron substituted C atom in the h-BNN sheet surface, and is unable to occur in the nitrogen substituted C atom. As large adsorption energy between the formed SO_3 with the C atom makes the process in the nitrogen substituted C atom cannot proceed to the next step.

As the process was performed at ambient conditions (25 °C, 1 atm), the enthalpy change for the SO_2 oxidation reaction is negative, indicating exothermic processes; and the Gibbs free energy is also negative, indicating that the oxidation of SO_2 is thermodynamically favored at normal condition. In relation to the effect of water for the other carbon sources, C-doped h-BNNS also show an increase in SO_2 oxidation with the presence of water, which is shown from the increase in the absolute values of Gibbs free energy and enthalpy changes of each reaction step. Nonetheless, even with the presence of water, SO_3 is still the final product of SO_2 oxidation, as the activation energy for the oxidation of H_2SO_3 is quite large — indicating that the process cannot proceed at normal temperature [47].

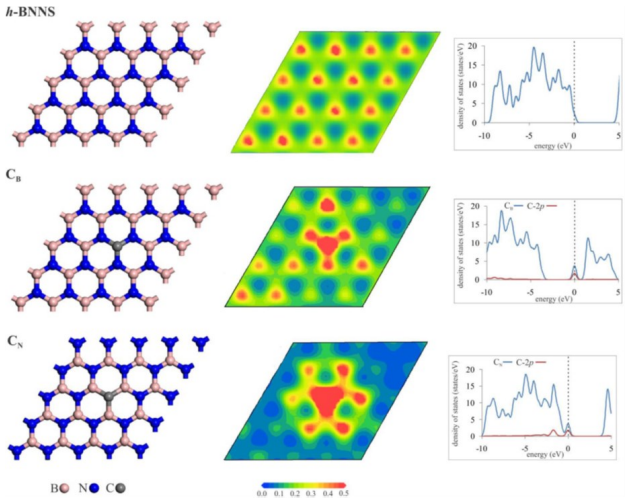

Figure 11. The structure (left), electron density map (middle), and DOS or PDOS plots of pristine and C-doped BNNSs for different Carbon-doped Boron Nitride structures. Note that the dashed line in the PDOS charts represents the Fermi level, which is set to zero [47]

Another type of boron nitride that has also been attracted attention is the carbon-doped fullerene-like boron-nitride nanocages ($B_{11}N_{12}C$ and $B_{12}N_{11}C$). The structures of $B_{11}N_{12}C$ and $B_{12}N_{11}C$ are shown in Figure 12. Overall, it has similar properties as the nanosheets, however, N_2O is required during the oxidation of SO_2 as an oxidant. The C-doping replaced a B and N atom of $B_{12}N_{12}$ with a C atom to obtain $B_{11}N_{12}C$ and $B_{12}N_{11}C$ nanoclusters, respectively. Upon replacing the B atom with a C atom, the atomic charges associated with the three neighboring N atoms become more negative, losing electronic charge, suggesting large surface reactivity. In comparison to the nanosheets, the calculated adsorption energy of SO_2 to the nanocages is −24.4 kcal/mol, which is smaller (less negative) than that of the SO_2 adsorption over the nanotubes. In regards to the SO_2 oxidation, it involves a two-stepwise reaction mechanism; which starts with the decomposition of N_2O into an activated oxygen atom (O*) and N_2 molecule, and followed by the oxidation of SO_2 by the O* species forming SO_3. It is also found that the existence of a C atom increases the catalytic activity of the BN nanocages for the decomposition of N_2O. Moreover, the adsorption energy of SO_3 on $B_{11}N_{12}C$ is calculated to be −8.2 kcal/mol, which means that SO_3 can be easily released from the $B_{11}N_{12}C$ surface and, hence, the catalyst may be renewed for the oxidation of another SO_2 molecule. Overall, $B_{11}N_{12}C$ is better than $B_{12}N_{11}C$, as the formed SO_3 would poison the $B_{12}N_{11}C$ nanocage and thus prevents the oxidation of the second SO_2 molecule over the surface [26]. A summary of carbonaceous materials for catalytic SO_2 oxidation is enumerated in Table 1.

3.2 Metal Oxides

Metal oxides play an important role in the field of catalysis. They are widely used as the main catalyst, co-catalyst, and support. The main content of metal oxide catalysis is the oxi-

dation reaction of catalysts composed of various metal oxides. The catalysts used in industry are mostly composed of a variety of metal oxides, among which transition metal oxides are the most common. This section uses the catalyst with metal oxide as the main catalytic active component to oxidize SO_2. Starting from metal oxides, such as V_2O_5/TiO_2, Pt/Pt alloys nanoparticle, Pt/γ-Al_2O_3, Fe_2O_3, α-Fe_2O_3/SiO_2, Pt/Pd, the influences of different catalysts on the oxidation reaction of SO_2 are explored.

3.2.1 V_2O_5/TiO_2 catalyst

In the early 20th century, vanadium pentoxide was used in the sulfuric acid industry as a metal oxide catalyst for the oxidation of SO_2 to SO_3. The V_2O_5-based catalysts are commercial catalysts currently used in SCR processes [50]. Supported V_2O_5/TiO_2 catalysts are widely used in catalytic reactions because of their excellent thermal stability and low oxidation activity. In this section, V_2O_5/TiO_2 is selected as the catalyst to explore the influence of this catalyst on the SO_2 oxidation reaction.

In the preparation of supported vanadium catalysts, the main synthesis methods include non-aqueous impregnation of vanadium alcohol and vanadium acetate, gas phase grafting of $VOCl_3$, aqueous impregnation of vanadium oxalate, dry impregnation of crystalline V_2O_5 [51] and thermal diffusion of crystalline V_2O_5 [52]. Vanadium oxalate water impregnation method is usually used in commercial preparations, which is mainly through TiO_2 powder and NH_4VO_3 aqueous solution in oxalate impregnated after drying, calcination, and other processes to prepare and obtain different content of catalysts [53]. Xiong *et al.* [54] also used catalyst preparation. As early as 1999, Dunn *et al.* [51] found that catalysts prepared by different initial synthesis methods all contained the same surface vanadium material due to the high mobility of V_2O_5 and the driving force of the system.

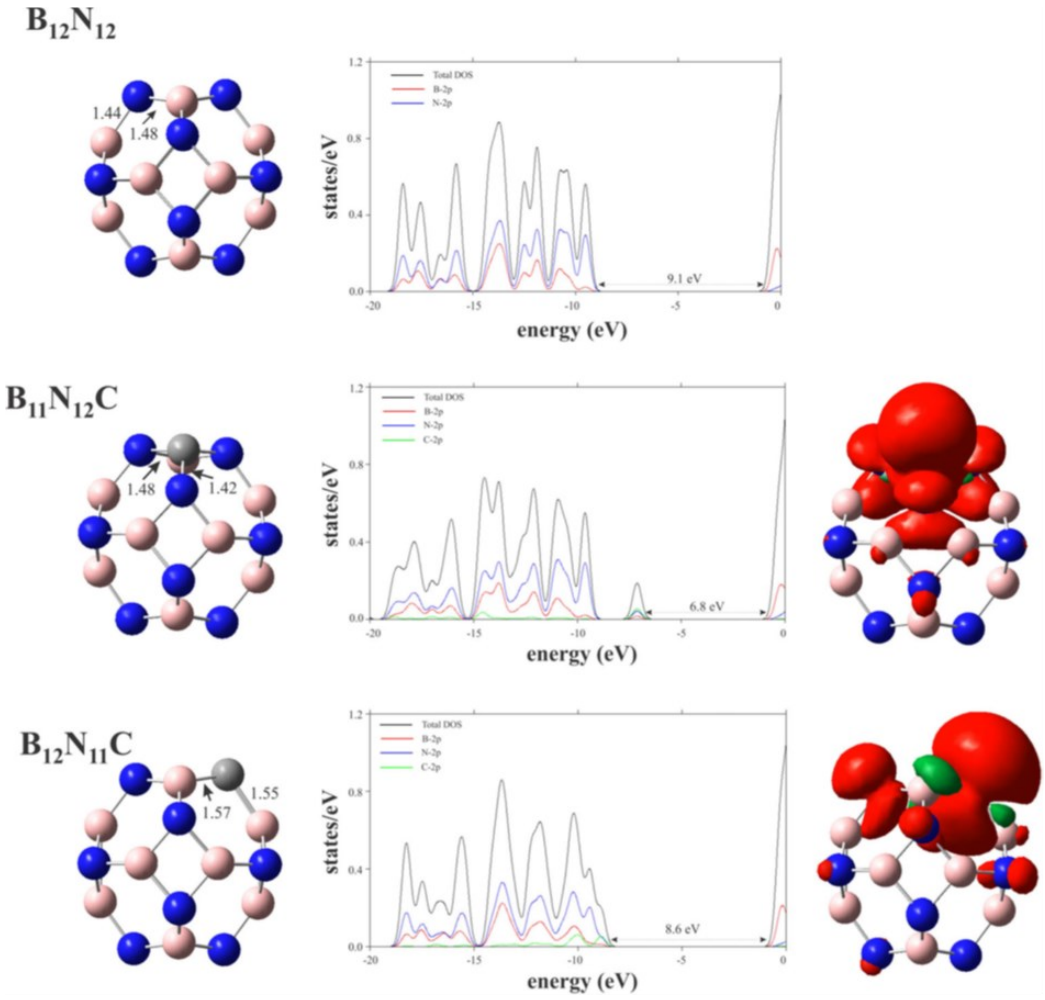

Figure 12. The structure (left), DOS plots (middle), and spin density isosurfaces of $B_{12}N_{12}$, $B_{11}N_{12}C$, and $B_{12}N_{11}C$ nanoclusters [48]. (Blue = N, Brown = B, Gray = C)

Table 1. Summary of carbonaceous materials for catalytic SO_2 oxidation

Catalysts	Oxidants	Synthesis Method	Reaction Temp. (°C)	Products		Adsorption Mechanism	Ref.
				SO_3	H_2SO_4		
Activated Carbon							
Activated Carbon	O_2 (Non-dissociated) attached to SO_2	Commercial	65	-	√	Eley-Rideal	[25,49]
V_2O_5/AC	O_2 (Non-dissociated)	Impregnation	100-250	-	√	Eley-Rideal	[37]
Microporous activated carbon fiber (ACF) and a microporous–mesoporous activated carbon fiber (Co-ACF),	O_2 (Dissociated)	Doping and Carbonization	-	-	√	Eley-Rideal	[36]
V_2O_5/AC	O_2 (Non-dissociated)	Impregnation and Calcination	-	-	√	Eley-Rideal	[34]
Activated Carbon	O_2 (Non-dissociated) as the oxidant shows a lower energy barrier to form SO_3	Demineralization	-	√	-	Langmuir-Hinshelwood	[35]
V_2O_5/AC	O_2 (Dissociated)	Impregnation and Calcination	120	-	√	Eley-Rideal	[38]
Carbon Nanotubes							
N-doped single-walled carbon nanotubes (SWCNTs), i.e. (6, 6)- and (8, 8)-SWCNTs	O_2 (Dissociated) is absorbed to the outer surface of the carbon nanotubes	Graphene Sheet Bending	-	-	√	Eley-Rideal	[39]
N-doped single-walled carbon nanotubes (SWCNTs), i.e. (6, 6)- and (8, 8)-SWCNTs	O_2 (Dissociated) is absorbed to the outer surface of the carbon nanotubes	Graphene Sheet Bending	-	√	-	Mars-van Krevelen	[41]
Red mud carbon nanotubes (RM-CNTs)	O_2 (Dissociated) is absorbed to the outer surface of the carbon nanotubes	Pyrolysis	140	√	-	-	[42]
Graphene Oxides							
Graphene Oxides (HO_OGP and 2HO_OGP)	O_2 (Dissociated)	Impregnation	-	√	-	Mars-van Krevelen	[43]
Graphene Oxides (GP, HO_GP, OGP, and HO_OGP)	O_2 (Dissociated)	Impregnation	20 -150	√	-	Mars-van Krevelen	[44]
Graphene Oxides (Soot)	O_2 (Dissociated)	Combustion and Atmospheric Photochemical Aging	-	√	-	Mars-van Krevelen	[45]
Pyridinic nitrogen (PyN)-doped graphene (GP)	-	PyN Substitution	20 -150	-	-	-	[46]
Carbon-doped Boron Nitride							
Carbon-doped fullrene-like boron nitride nanocages ($B_{11}N_{12}C$ and $B_{12}N_{11}C$)	Activated Oxygen atom (O^*) from N_2O	Carbon Substitution	25 (Room Temperature)	√	-	Langmuir-Hinshelwood	[48]
Carbon-doped hexagonal boron nitride nanosheets (h-BNNSs)	Activated Oxygen atom (O^*) from O_2	Carbon Substitution	-	√	-	Langmuir-Hinshelwood	[47]

To fully understand the factors affecting supported vanadium catalysts, various characterization techniques were used to find that the surface structure and oxidation state of vanadium on various supports are dynamic and strongly dependent on the specific environment [51]. When exploring the supported vanadium catalyst, it was found that the surface vanadium material has the properties of both Lewis and Brønsted acids, and the ratio of Brønsted and Lewis acids increases with the increasing of the surface vanadium coverage rate [51]. The Brønsted acid site is conducive to the adsorption of SO_2 [50]. However, the total number of acid centers on the surface was not related to the coverage of metal oxides on the surface [52]. Topsøe *et al*. [55] found that the Brønsted acid center is the active center of catalysis. Subsequent studies [53,55] found that the V-OH group was responsible for the acidity of the V_2O_5/TiO_2 catalyst Brønsted by means of infrared spectroscopy (DRIFT).

Metal oxide additives are divided into non-interacting additives and interacting additives. The former can indirectly affect the molecular structure of vanadium through lateral action, while the latter can affect the length of the V-O bond in the molecular structure of the catalyst or the formation of crystallization of mixed metal oxidation relative to the catalyst [51].

Water affects the activity of the catalyst. By changing the temperature conditions, it is pointed out that the surface vanadium material can still retain its structure above 300 ℃, while at about 200 ℃ and below, the water adsorbed on a single layer is exist on the V_2O_5/TiO_2 catalyst and widely dissolve the surface vanadium material [51]. This also confirms that the presence of water vapor could affect the surface vanadium of the V_2O_5/TiO_2 catalyst. In the study on the influence of water on the catalyst, it was mentioned that the interaction between water and catalyst surface changed the distribution of active sites and Lewis and Brønsted acid sites on the catalyst surface. Especially for sulfated V_2O_5/TiO_2, the presence of water will also increase the number of Brønsted acid centers on the surface [56].

Under the background of selective reduction (SCR), the experiments of ammonia and NO on the surface and the FTIR studies show that NH_3 is easily adsorbed on V_2O_5/TiO_2 catalyst and exists in the form of NH_3* and NH_4^+* on the surface Lewis acid site and Brønsted acid site, respectively [3]. Water significantly converts surface NH_3* species to surface NH_4^+* species by hydrolyzing vanadium sites on the surface and at high temperatures (≥ 250 ℃). He *et al*. [57] also found the same situation with V_2O_5-5%WO_3/TiO_2 as a catalyst. However, the adsorption of NO on the V_2O_5/TiO_2 catalyst is weak or even non-adsorption, the main reason is that surface ammonia ions hinder the adsorption of NO, so NO has little influence on the catalyst [56].

The Redox performance of TiO_2-supported metal oxide catalyst was studied by partial oxidation of methanol to formaldehyde. The trend shows that V_2O_5/TiO_2 has surface redox sites, so the SO_2 oxidation reaction can be effectively catalyzed [51]. There are few studies on the oxidation of SO_2 on supported vanadium catalysts from the perspective of molecular structure and reactivity. The research by Dunn *et al*. [51] mainly focuses on the influence of various bonds existing in molecules on reactions. In particular, he mentioned that the bridging V-O-V bond and the terminal V=O bond do not play a key role in the overall kinetics of SO_2 oxidation. Primary Raman studies have shown that an increase in the surface coverage range of surface vanadium does not increase the oxidation conversion frequency (TOF) of SO_2, which means that only one surface vanadium site is required for SO_2 oxidation. The significant relationship between SO_2 oxidation and the V-O-M bridge bond is demonstrated by changing the ligand of a specific oxide carrier to change the turnover frequency by more than an order of magnitude. The more basic the bridging V-O-M bond is (the lower the electronegativity of the oxide carrier), the higher the activity of SO_2 adsorption and subsequent oxidation of acidic SO_2 molecules. Otherwise, it inhibits the adsorption and oxidation of SO_2 [51].

The properties of metal oxide additives are the key factors affecting the supported vanadium catalyst. It has been reported in the literature that interacting additives negatively affect the conversion frequency of SO_2 oxidation on V_2O_5/TiO_2 catalysts [51]. Non-interacting additives provide additional surface sites for SO_2 oxidation, this effect can be sustained only when the total surface coverage of the additive is less than that of the monolayer and the oxidation activity of the additive is greater than that of the supporting oxide covered by it [51].

Under the condition of dehydration, the surface sulfate on the sub-monolayer vanadium catalyst preferentially coordinates with the oxide support and participate in the redox cycle, which can promote the oxidation of SO_2 at high temperature, but the surface sulfate might evaporate with the increase of temperature.

However, at lower temperatures (< 400 ℃), the rate at which sulfates undergo redox cycles is not obvious [51].

Through the analysis of SO_2 and its product SO_3, it is found that SO_2 and SO_3 compete to adsorb on the surface vanadium and SO_3 will be preferentially adsorbed, resulting in a stronger binding between SO_3 and the surface vanadium. Under this premise, it can be considered that the partial pressure dependence of rate on SO_2 and SO_3 is of the first order and negative order respectively [51]. Lai *et al.* [56] also mentioned the zero-order dependence of O_2 on this basis.

Dunn *et al.* [51] mentioned in the literature that when the change of O_2 partial pressure exceeds 1 vol.%, the reaction rate is independent of the gas-phase oxygen partial pressure. Xiong *et al.* [54] also concluded that the reaction order is about 0. When the O_2 partial pressure is 0.1–1 vol.%, the oxidation rate depends on the gas phase oxygen partial pressure by about half an order of magnitude. Similarly, the research on the influence of oxygen-oxygen atoms in V_2O_5 also participated in the oxidation of SO_2 [54]. It is worth mentioning that O_2 did not directly participate in the formation of SO_3, but promoted the formation of intermediate products ($VOSO_4$ and HSO_4^-) and indirectly accelerated the reaction [58]. As O_2 concentration increases, SO_3 concentration also increases.

The possible location of SO_2 adsorption on the VO_X/TiO_2 catalyst was explored. Loading vanadium on TiO_2 significantly weakens the adsorption of SO_2 [50], owing to the enhanced acidity on the surface of loaded vanadium hinders the adsorption of acidic SO_2. In addition, the reaction of SO_2 with vanadium monomer and vanadium dimer was discussed [50]. Based on the calculation of periodicity and cluster, it is found that sulfation is the preferred way for SO_2 oxidation on vanadium monomer. The energy distribution shown in Figure 13 (a) and (b) proves that Ti-OH can promote the reaction with SO_2. For vanadium dimers, there is almost no active oxidized SO_2 in either the V-O-V or V-O-Ti structure. However, it is worth mentioning that SO_2 can be oxidized on vanadium dimer through sulfation, although this method is not as easy as SO_2 oxidation on vanadium monomer [50].

It is necessary to study the effect of water vapor on the reaction. Adding water to the reaction mixture (containing SO_2, SO_3, and O_2) can observe that the conversion of SO_2 on the V_2O_5/TiO_2 catalyst decreases, and the inhibition effect of water may be greater at a higher temperature. Dunn and his collaborators [51] speculated that the inhibition of water might be related to the adsorption of SO_3 or the reversible site blockage of the oxidized surface vanadium active site, which was confirmed [54]. There is competitive adsorption between H_2O and SO_3, which can be confirmed by adding H_2O to the reaction. The concentration of SO_3 increases rapidly from 11 ppm to 23 ppm and then decreases gradually to 8.5 ppm. When H_2O stops adding to the reaction, the concentration of SO_3 rapidly drops to nearly 0, then returns to 12 ppm and remains constant. The reason is that more active centers are released by desorption. At this time, more SO_3 is adsorbed, so the concentration of SO_3 decreases [54]. In 2018, it was reported that water improved SCR selectivity by reducing the formation of N_2O in the V_2O_5/TiO_2 catalyst. However, the role of water in SCR is still unknown [56].

The research on catalyst oxidation of SO_2 is often carried out around the denitration application of SCR. A series of related studies have mentioned the influence of nitrogen-containing

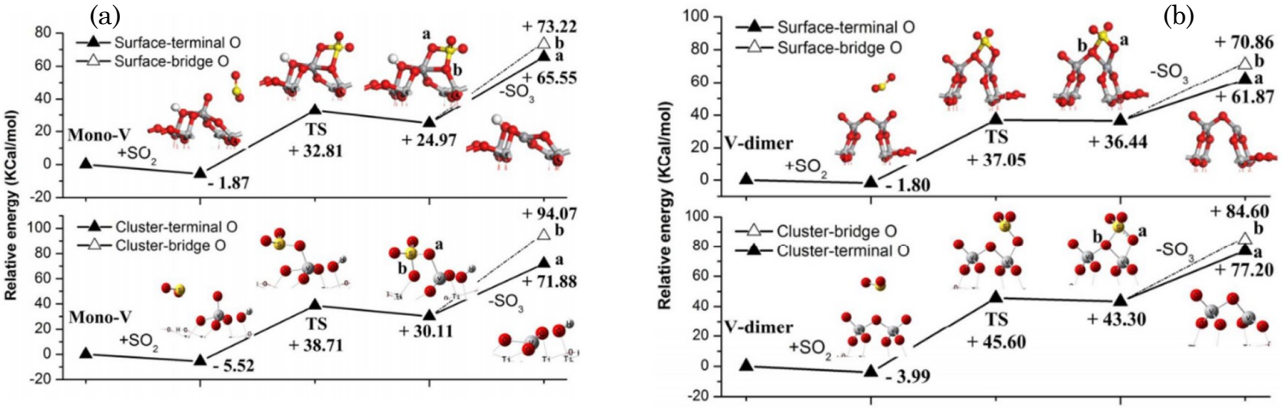

Figure 13 The sulfation pathway of SO_2 interacts with vanadia oxo-site [50] (a), or vanadia dimer [50] (b)

substances on SO_2 oxidation reactions. Svachula *et al*. [59] conducted a detailed study on NH_3 and NO. The results showed that low concentration NH_3 (~100 ppm) was added to the reaction stream to form ammonia and strongly inhibited the oxidation of SO_2 at 330 ℃. For this result, it is hypothesized that NH_3 or H_2O had no significant effect on SO_2 oxidation and gave the same explanation as water inhibition [54]. There is also competitive adsorption between NH_3 and SO_3 to inhibit the desorption of SO_3 and promote the adsorption of SO_2. Among them, NH_3 inhibits the formation of SO_3 more significantly than H_2O [54]. Although NO has no obvious effect on the SO_2 oxidation activity of the catalyst [51], the addition of NO and NH_3 provides oxygen for the catalyst surface, which is conducive to the oxidation of SO_2 [58]. In addition, the investigation found that NO_x can significantly promote SO_2 oxidation by acting on the catalyst surface, and the effect of NO_x on vanadium valence is generally more significant than NH_3 and H_2O [54].

Although the oxidation of O_2 is an exothermic reaction, the temperature increase is conducive to the formation of SO_3 [54]. Analysis of the rate and temperature image as shown in Figure 14 (a) and (b) shows that under various V_2O_5 loads, the oxidation rate of SO_2 increases with the increase of temperature, and reaches saturation at high values [53]. Qing *et al*. [58] believes it is related to the increase of V^{5+} and V^{4+} conversion. Temperature can affect reactions in other ways, too. At temperatures above 200 ℃ and in the presence of O_2, SO_3 substances exist in the form of SO_4 substances with more thermodynamic stability through conversion. On the contrary, in the absence of O_2, SO_2 adsorbs on TiO_2 by physical adsorption (SO_2) or chemical adsorption (SO_3), and the ratio of surface material forms depends on the adsorption temperature [56].

Under actual industrial SCR conditions, vanadium can be deposited directly on the catalyst surface if the fuel contains vanadium compounds. With the increase of V_2O_5 loading on the surface of the catalyst, the oxidation rate of SO_2 may also increase. However, once the bulk structure of the catalyst is formed (greater than 5.7 wt.%), the oxidation rate of SO_2 reaches saturation with the further increase of vanadium concentration. The saturation oxidation rate measured at 733 K is about 1×10^{-3} $\mu mol.m^{-2}.s^{-1}$ [53].

3.2.2 Other catalysts (Pt and Pt alloys nanoparticles, Fe_2O_3, $Pt/\gamma\text{-}Al_2O_3$, $\alpha\text{-}Fe_2O_3/SiO_2$, and Pt/Pd)

The use conditions of V_2O_5 catalyst should meet the requirements under high temperature conditions, and research showed that vanadium pentoxide is a carcinogen [60]. Before the introduction of vanadium-based catalysts, platinum was the main catalytic unit in the SO_2 conversion process. Now, to reduce the pollution of SO_2 to the environment, researchers have started to study platinum-based catalysts, especially platinum-based catalysts containing rhodium [61] and $Pd\text{-}Pt/Al_2O_3$ catalysts [33]. Although noble metal catalysts can avoid

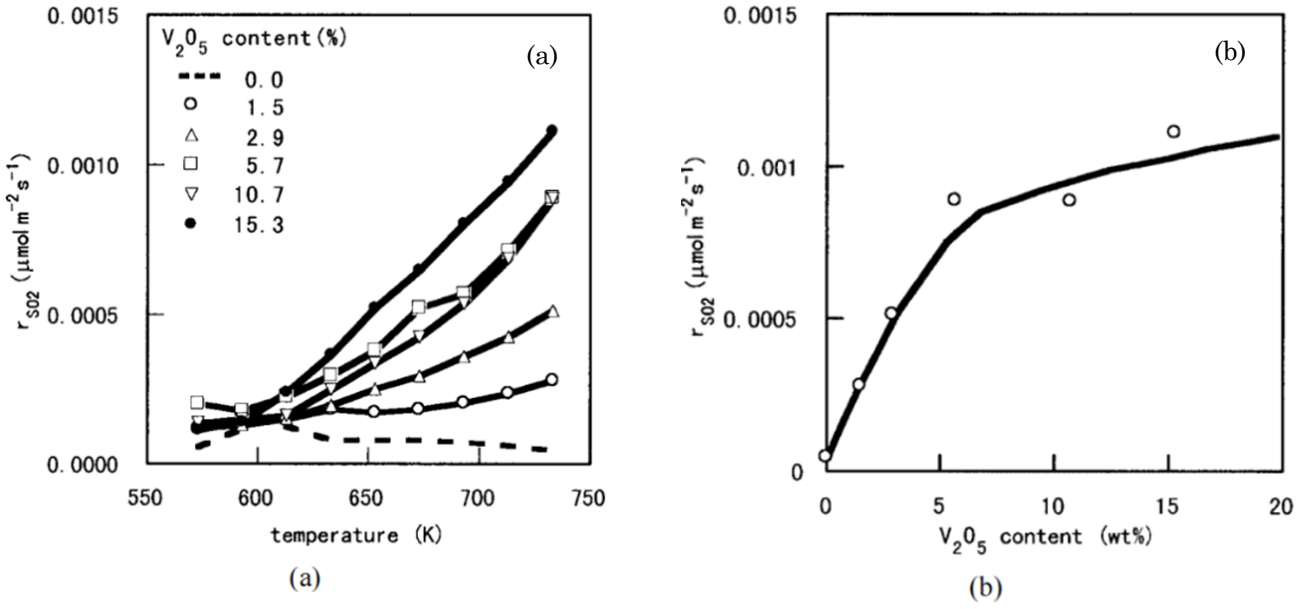

Figure 14. (a) Change of SO_2 oxidation rate under different V_2O_5 loads and changing temperature [53]; (b) Dependence of oxidation rate on V_2O_5 load at 733 K [53]

the problem of vanadium pentoxide, they are expensive and easy to be polluted, thus researchers began to look for low-temperature active, environmentally friendly, and cheap catalysts, such as iron oxide and related catalysts. As with vanadium-based catalysts, platinum catalysts and controlled pore glass silica (CPG)-supported pure palladium and rhodium samples [61], Pd−Pt/Al_2O_3 catalyst, α-Fe_2O_3/SiO_2 and Co_3O_4-CeO_2-α-Fe_2O_3/SiO_2 nanocatalyst were synthesized by wet impregnation [62].

The catalytic oxidation strength of metal oxides is related to specific surface area, surface porosity, particle size and performance [63]. Highly active catalysts often have good dispersion and small particle size as demonstrated by Koutsopoulos *et al*. [61]. Notably, they also found that the presence of dopants (palladium and rhodium) in the catalyst samples have significantly enhanced the activity of the catalyst. The characterization of Fe_2O_3 showed that both micro-scale and nano-scale Fe_2O_3 have hexagonal structures [60]. Based on the Fe_2O_3 catalyst, promoters such as rare earth metals, transition metals, and lanthanide metals are added to the Fe_2O_3 catalyst to improve the efficiency of SO_2 oxidation. In particular, the cerium element provides stability for the catalyst and reduces the activation energy [62]. In 1979, researchers found that bimetallic catalysts were more active than single metals in the oxidation of SO_2 and the formation of SO_3 [15].

The Fe_2O_3 catalyst was tested in the temperature range of 100–1000 ℃ [60]. It was found that its activity increased with temperature, significantly enhanced the oxidation of SO_2 and nanoscale Fe_2O_3 was more effective than microscale Fe_2O_3. Similarly, the maximum catalytic activity of the platinum catalyst is observed in the temperature range of 250–700 ℃, and the activity will decrease with the further increase in temperature, which may be due to the sintering of active particles [61]. Koutsopoulos *et al*. [61] also mentioned the possibility of the influence of thermodynamic equilibrium limitation. Different from the platinum catalysts (the maximum activity temperature is 510 ℃), the maximum activity temperature of pure palladium (Pd/CPG) and rhodium (Rh/CPG) catalysts is higher, and both are 650 ℃.

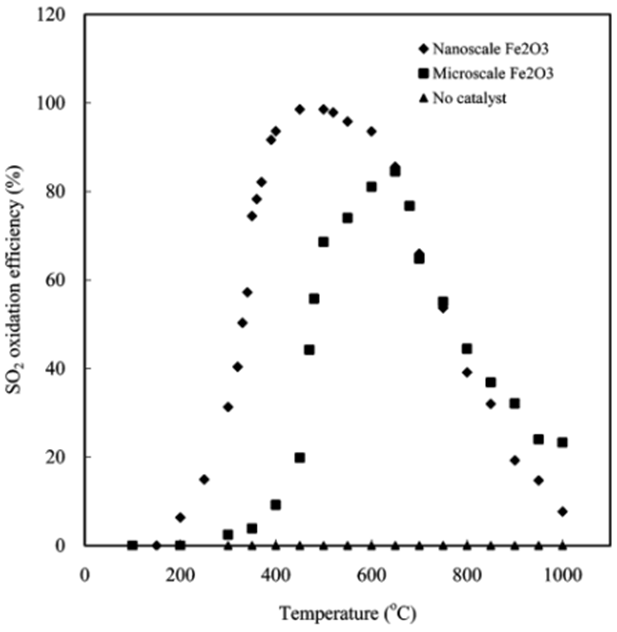

Figure 15. Effect of temperature on the oxidation efficiency of SO_2 catalyzed by micron and nanometer Fe_2O_3 [60]

At given flow rates of 30, 40, 50, 60, and 70 mL/min, it was found that the oxidation efficiency of SO_2 with nanoscale and microscale Fe_2O_3 catalysts was not affected by flow rate, although their specific surface areas were quite different [65]. The experimental investigation found that the catalytic activity of all the prepared catalysts (α-Fe_2O_3/SiO_2 and Co_3O_4-CeO_2-α-Fe_2O_3/SiO_2) can be enhanced with the increase of SO_2 concentration until the concentration of SO_2 is greater than a certain volume, and the activity of the catalyst is stable [65].

The reduction of catalyst sample size could prompt to the oxidation of SO_2 [62]. It was found that micro-scale Fe_2O_3 with a specific surface area of 4.0 m^2/g and nanoscale Fe_2O_3 powder with a specific surface area of 240.0 m^2/g could promote SO_2 conversion. Comparing the effects of microscale and nano-scale Fe_2O_3 on SO_2 oxidation rate in the temperature range of 100-1000 ℃, it is found (Figure 15) that nano-scale Fe_2O_3 can almost completely oxidize SO_2 at 450 ℃, while the oxidation efficiency of micro-scale Fe_2O_3 at higher temperatures (650 ℃) is still lower than that of nanoscale Fe_2O_3. This shows that nano Fe_2O_3 can better reduce the activation energy. In other words, a high specific surface area is conducive to the reaction [60].

The conversion rate of SO_2 oxidation is dependent on the reaction temperature, which is affected by factors such as gas flow rate and catalyst loading of the active phase [61]. In the study of SO_2 oxidation on Pt/γ-Al_2O_3 catalyst, researchers mainly focus on the influence of temperature. At temperatures below 300 ℃, SO_2 is sensitive to adsorption, desorption, and surface reaction [66]. With the increase in temperature, the coverage rate of SO_3 decreases, and the adsorption, desorption, and reverse surface reactions of O_2 are faster, and O_2 is

dominant on the surface of Pt. However, when the temperature is higher than 500 ℃, the oxygen coverage rate decreases due to the increase in vacancy density [66]. It can be directly observed in Figure 16 that the conversion of SO_2 increases with temperature, ranging from 380 to 700 ℃. It is worth noting that the conversion rate decreases with a further increase in temperature when the temperature reaches above 500 ℃ [62]. Yan *et al*. [62] speculated that this may be due to the limitation in thermodynamic equilibrium and the sintering of nano-Fe_2O_3 at high temperatures.

SO_3 inhibits SO_2 oxidation by occupying the active site of oxygen adsorption, and the inhibition effect is not linear [66]. It is worth paying special attention that when SO_3 is present in the feed and the temperature is lower than 300 ℃, SO_3 occupies most of the active sites, which inhibits the oxidation of SO_2, and the inhibition degree does not change significantly with the increase of SO_3. On the contrary, when there is no SO_3 in the feed, its inhibition is small [66]. The evaluation experiment was conducted with SO_3 containing 125 ppm concentration (excessive) and SO_2 containing 50 ppm concentration, and it was concluded that excessive SO_3 product would inhibit the oxidation of SO_2 [33].

The effect of changing the oxygen concentration on the oxidation of SO_2 over the single metal catalyst was evaluated. The results show that changing the oxygen concentration does not significantly affect the reaction of Pt and Pd catalysts [33]. However, for bimetallic catalysts, the raw material containing O_2 can enhance the oxidation of SO_2. In another test, the concentration of O_2 is set as a constant value, and the temperature varies in the range of 150–450 ℃. Increasing the concentration of

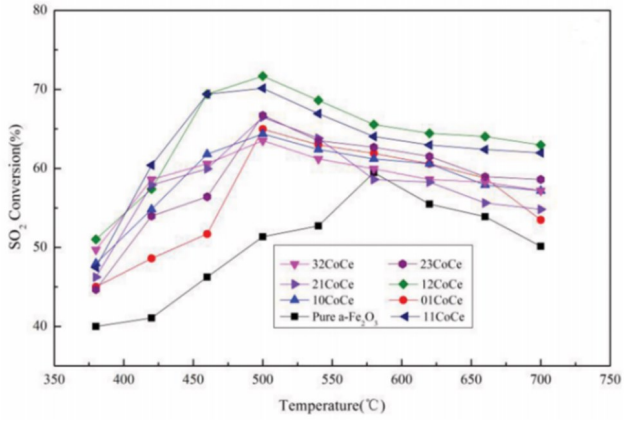

Figure 16. Effect of various cobalt and cerium promoters on SO_2 conversion at different temperatures from 380 ℃ to 700 ℃ [62]

SO_2 leads to an increase in the SO_2 conversion rate of Pt/Al_2O_3 and Pd/Al_2O_3, and the conversion frequency of Pt/Al_2O_3 is higher than that of Pd/Al_2O_3 under the same conditions. For example, at 50 ppm Pt and 50 ppm Pd, the TOF of Pt/Al_2O_3 is about 20 s^{-1}, while the TOF of Pd/Al_2O_3 is about 2.2 s^{-1}. In other words, Pt is more active in oxidizing SO_2 [33].

X-ray diffraction analysis of α-Fe_2O_3 catalysts with different Co and Ce ratios showed that the 12CoCe catalyst showed better crystallinity of α-Fe_2O_3, which means that it can enhance the stability of the catalyst and promote the oxidation of SO_2 [62]. Containing Co and CeO_2 promoters α-Fe_2O_3/SiO_2 catalyst just meets the above-mentioned goal of promoting SO_2 oxidation to SO_3. The pure α-Fe_2O_3 could only function well at a higher temperature of 580 °C, with less than 59.5% SO_2 conversion. By adding the cobalt and cerium with the ratio of 12, the temperature was successfully lowered down to 500 °C with 71.6% SO_2 conversion [62].

What is different is that Liu et al. [63] found that fly ash can catalyze the formation of SO_3 or absorb SO_3, depending on the temperature and alkalinity of fly ash. The presence of copper smelting dust affects the conversion of SO_2 on Fe_2O_3 and CuO catalysts. Fe_2O_3 catalyst has been mentioned many times in the literature [63]. For example, Fe_2O_3 has a strong effect on SO_2 oxidation.

4. Process Engineering Design and practice

The selection of the reactors used for SO_2 oxidation is as critical as the selection of catalysts. The reactor was coupled with an electric heating device to maintain a constant temperature and connected to the FT-IR gas analyzer to determine the composition of gas leaving the reactor. The whole experiment apparatus for the SO_2 removal included the gas cylinders, valves, mass flow controllers, and a gas mixer (as shown in Figure 17 (a)) [25,67]. The flue gas analyzer is also added to some of the systems for measuring the change in SO_2 concentration [34,37], and one of the apparatuses is shown in Figure 17 (b) [38].

The present study concerns the design of the reactor for the commercialization of a novel process. Although a quartz reactor has been considered for this purpose, its implementation on a large scale would be prohibitively expensive. As an alternative, the use of stainless steel has been proposed. However, the use of stainless steel could cause corrosion due to the

production of sulfuric acid resulting from the oxidation of SO_2. Scientific community is still finding effective solutions for this hurdle. It is worth noting that the addition of a pH-balancing substance, such as NaOH, is a common industry practice when acid is produced during a reaction. However, since the H_2SO_4 produced during SO_2 oxidation is proposed to be extracted and utilized, the addition of a pH-balancing substance may require additional processing, resulting in increased costs.

The effectiveness of the currently applied lab-scale fixed bed reactor with a single catalyst bed would decrease as the size increases. Moreover, the use of a fixed bed reactor suggests several drawbacks that could reduce the SO_2 removal efficiency. The application of a fixed bed could lead to hot spots in the reactor, lowering the reaction efficiency. Thus, a multi-parallel stainless-steel tube with multiple horizontal catalyst beds is suggested to enhance the efficiency of the processing system. The occurrence of hot spots could be reduced by filling the catalyst in varied ratios inside the multiple horizontal beds. The bed closest to the air inlet should have the lowest concentration of catalyst, and increase the concentration in each bed as the air flows throughout the reactor. Thus,

(a)

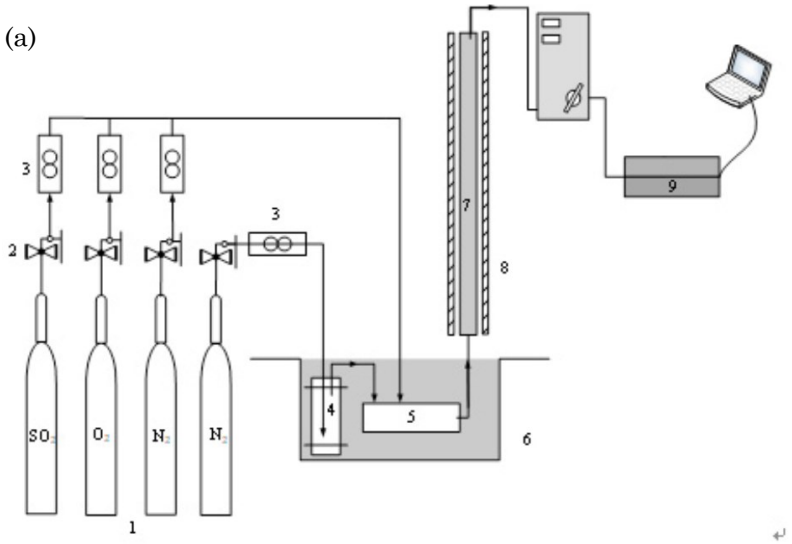

Gas cylinder; (2) Valve; (3) Mass flow controller, (4) Water; (5) Gas mixer; (6) Water bath; (7) Reactor; (8) Electric heating device; (9) FT-IR gas analyzer

(b)

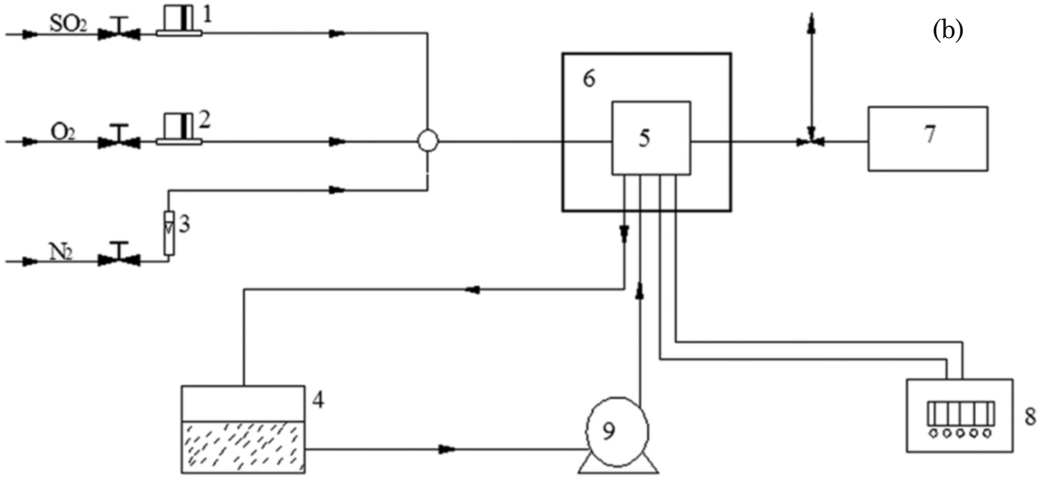

(1) and (2) mass flow controller; (3) rotameter; (4) cooling water; (5) sample chamber of the FTIR spectrometer; (6) high pressure/high temperature chamber of the diffuse reflectance accessory; (7) sweep gas analysis meter; (8) temperature controller; (9) water pump

Figure 17. (a) SO_2 removal experiment apparatus [25,67], (b) SO_2 removal experiment apparatus with flue gas analyzer [38]

an isothermal condition across the height of the reactor could be maintained. Moreover, the pressure drops throughout the reactor can cause channeling which will also reduce the SO_2 removal efficiency. Maintaining an identical pressure drop across the reactor is vital to achieve the desired conversion of SO_2 and avoid hot spots in certain parts of the reactor. The most optimal solution to these problems is by using a real-time digital data analysis which could alternate the reactor parameters to achieve the maximum conversion. Thus, a stable reactor operation can be achieved as well as reducing the possibility of reaction runaway through predictive modeling of the reaction process [68].

The application of a better reactor design could further improve the reaction efficiency and ease the scale-up process of the lab-scale reactors. The fluidized bed reactor is one of the reactors that can be considered due to its several advantages over the traditional fixed bed reactor (Table 2). Constant catalyst fluidization increases the mass and heat transfer of the process, improving the reaction rate. Moreover, the most concerning disadvantages of the fixed bed reactor, such as its high-pressure drop, channeling, and the occurrence of hotspots, can be eliminated by using the fluidized bed reactor. Even though the catalysts' constant fluidization will reduce the catalysts' retention and leads to frequent maintenance, the ability to control the reactor temperature surmounts its drawbacks. With the exothermic adsorption reaction of SO_2 removal, efficient temperature control is crucial to avoid reaction runaway and catalyst damage. Therefore, the commercialization of the SO_2 mitigation process should highly consider the use of an industrial-scale fluidized bed reactor, as shown in Figure 18.

Table 2. Comparison of fixed bed reactors and fluidized bed reactors [69–72]

Parameters	Fixed Bed Reactor	Fluidized Bed Reactor
Catalyst Loading	Catalysts remain stationary throughout the reaction process	Catalysts continuously fluidized and circulated throughout the reaction
Air Flow Regime	Laminar One-Way	Turbulent Circulation
Mixing	Worse	Better
Mass and Heat Transfer Efficiency	Worse	Better
Pressure Drop	Significant	Insignificant
Reaction Rate	Slower	Faster
Catalyst Retention	Better	Worse
Hotspots Occurrence	Likely	Unlikely
Temperature Control	Difficult	Easy
Channeling	Occur	Do not occur
Maintenance	Minimal	Frequent
Scale-up	Easy	Difficult
Catalyst Regeneration	Difficult	Easy

Fixed bed and fluidized bed reactors are generally used in the SO_2 oxidation. Till date, there is no optimal reactor that could be recommended because each of these reactors confers pros and cons when dealing with highly exothermic reaction and intrinsic equilibrium limitations (refer to Table 2). Despite this, the fixed bed reactor gains more attention in industries because its ease to scaling up the process. The multiple catalytic bed in series is designed to enhance SO_2 conversion while mitigating the impact of equilibrium limitations. The temperature could be more effectively controlled through installation of pre-cooling system between the two-bed, three-bed or four-bed catalytic systems to extract excess heat to a greater extent, hence enhancing the conversion rates.

5. Challenges and Future Prospects

Even though a great deal of research has been executed to determine the possibility of SO_2 removal using these catalysts, only some measure the removal efficiency and the recyclability of the catalysts that are significant for large-scale applications. Until now, most research still focuses on whether the proposed catalysts can be used for SO_2 mitigation. Future research should focus on measuring the catalyst stability and recyclability, especially

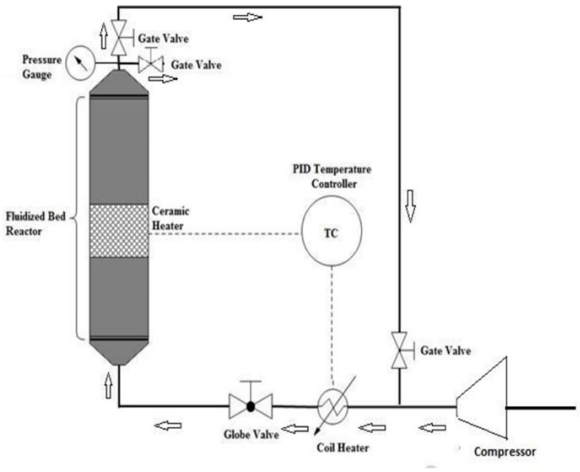

Figure 18. Sample of fluidized bed reactor schematic diagram [73]

with the possibility of deactivation by sulfur or coke. Scaling-up of the process should also take into account the other pollutants or gases that exist in the environment, and whether these gases will affect the catalytic SO_2 oxidation process. An initial study on the effect of the SO_2 catalysis process with the presence of foreign gases that mimics the gases from industries can be considered before deciding to scale up the process.

The not yet agreed-on mechanism of SO_2 removal using these catalysts also hinders the improvement of the process, as several reaction pathways occurred that lead to the same SO_2 catalytic oxidation process. Various researchers used different methods in determining the reaction pathway, such as the thermogravimetric analysis [25], projected density of states (PDOS) [35], temperature-programmed decomposition (TPDC) experiment [37], high-precision conductometer [36], and Fourier transform infrared (FTIR) analysis [34,38]. Therefore, joint research to find the exact mechanism of SO_2 oxidation in a particular catalyst that complies with all methods to determine the reaction pathway can be conducted to pave a clear path toward the improvement of the process.

Most of the research is also fixated on activated carbon and V_2O_5/TiO_2; however, considering the other promising properties of materials should be urged. Considering the urgency of this matter, future research may focus on understanding the specific mechanism of SO_2 removal in catalysts, and start experimenting with mimic gases to simulate real environmental conditions, before designing the most efficient reactor design for the process.

6. Conclusions

Various carbonaceous catalysts were considered for SO_2 mitigation via catalytic oxidation. Activated carbon, carbon nanotubes, graphene oxide, and carbon-doped boron nitride are all relevant to be used for SO_2 removal. In addition, V_2O_5/TiO_2 is used as the main representative catalyst for the oxidation reaction of SO_2 catalyzed by metal oxide-typed catalyst, which is mainly divided into two parts for discussion: V_2O_5/TiO_2 catalysts and other catalysts (Pt, Pt/Pd, Pt/γ-Al_2O_3, Fe_2O_3, α-Fe_2O_3/SiO_2, and CuO, etc.), detailed summary of the performance of different catalysts and SO_2 oxidation reaction factors, such as temperature, pH, concentration, water and other substances.

The conversion of SO_2 to SO_3 is a significant industrial process used in the production of H_2SO_4. The choice of catalyst for this reaction is crucial for optimizing SO_2 conversion rate in conjunction with minimizing the environmental impact. Activated carbon shows large surface area with its porous structure, and catalytically active as embedded with metal oxides. It gives bifunctionality, where SO_2 adsorption on the activated carbon and further catalytic oxidation on the embedded metal oxides. Carbon nanotubes display unique electronic properties and graphene oxide decorated with oxygenated functional groups, both could be an effective catalyst by tailoring the specific functionalization and reaction conditions. Carbon-doped boron nitride is an emerging material due to carbon incorporated into the alternating boron and nitrogen atoms provides catalytic active sites, a high thermal and mechanical stability, electrical and chemical properties for SO_2 oxidation. Compared to V_2O_5-based materials, the carbonaceous materials have just been sprouting out in recent years. V_2O_5-based materials have been intensively used in industries due to its robustness at temperature range between 400 and 600 ^oC and pressures around 1–2 atm. The industrial conversion of SO_2 to SO_3 for the production of H_2SO_4 using vanadium oxide-based catalysts could approaching nearly 90% and above.

We envisage that the findings of this study could help to establish an innovative path for future SO_2 removal prospects, meanwhile advancing the catalysts designs and utility. All in all, this research would be merits for human health and environmental sustainability.

Acknowledgments

The work is supported by the Ministry of Higher Education through the Fundamental Research Grant Scheme (FRGS/1/2019/TK02/XMU/03/1), Xiamen University Malaysia Research Fund (grant number: XMUMRF/2019-C4/IENG/0019 and XMUMRF/2020-C5/IENG/0029).

CRediT Author Statement

Tanoko Matthew Edward: Validation, Investigation, Writing - Original Draft, Visualization; Ying Weng: Validation, Investigation, Writing - Original Draft, Visualization; Sin Yuan Lai: Conceptualization, Methodology, Validation, Investigation, Writing - Review & Editing, Visualization, Supervision, Project administration, Funding acquisition. All authors have read and agreed to the published version of the manuscript.

References

[1] Nguyen, H.H., Gyawali, G., Martinez-Oviedo, A., Nguyen, H.P., Lee, S.W. (2020). Modified blue TiO_2 nanostructures for efficient photo-oxidative removal of harmful NOx gases. *Korean Journal of Chemical Engineering*, 37(9), 1507–1514. DOI: 10.1007/s11814-020-0560-z.

[2] Zhang, X., Wang, J., Chen, D., Liu, L. (2021). The adsorption performance of harmful gas on Cu doped WS2: A first-principle study. *Materials Today Communications*, 28 DOI: 10.1016/j.mtcomm.2021.102488.

[3] Lv, W., Fan, X., Gan, M., Ji, Z., Chen, X., Yao, J., Jiang, T. (2018). Investigation on activated carbon removing ultrafine particles and its harmful components in complex industrial waste gas. *Journal of Cleaner Production*, 201, 382–390. DOI: 10.1016/j.jclepro.2018.08.064.

[4] Huang, Y., Su, W., Wang, R., Zhao, T. (2019). Removal of typical industrial gaseous pollutants: From carbon, zeolite, and metal-organic frameworks to molecularly imprinted adsorbents. *Aerosol and Air Quality Research*, 19(9), 2130–2150. DOI: 10.4209/aaqr.2019.04.0215.

[5] Khan, M.A., Ngo, H.H., Guo, W., Liu, Y., Zhang, X., Guo, J., Chang, S.W., Nguyen, D.D., Wang, J. (2018). Biohydrogen production from anaerobic digestion and its potential as renewable energy. *Renewable Energy*, 129, 754–768. DOI: 10.1016/j.renene.2017.04.029.

[6] Kumar, G., Kim, S.H., Lay, C.H., Ponnusamy, V.K. (2020). Recent developments on alternative fuels, energy and environment for sustainability. *Bioresource Technology*, 317 DOI: 10.1016/j.biortech.2020.124010.

[7] Tarhan, C., Çil, M.A. (2021). A study on hydrogen, the clean energy of the future: Hydrogen storage methods. *Journal of Energy Storage*, 40 DOI: 10.1016/j.est.2021.102676.

[8] Singh, S., Ru, J. (2022). Accessibility, affordability, and efficiency of clean energy: a review and research agenda. *Environmental Science and Pollution Research*, 29(13), 18333–18347. DOI: 10.1007/s11356-022-18565-9.

[9] Dahiya, S., Anhäuser, A., Farrow, A., Thieriot, H., Kumar, A., Myllyvirta, L. (2020). Ranking the world's sulfur dioxide (SO_2) hotspots: 2019-2020

[10] Montzka, S.A., Dlugokencky, E.J., Butler, J.H. (2011). Non-CO_2 greenhouse gases and climate change. *Nature*, 476(7358), 43–50. DOI: 10.1038/nature10322.

[11] Sudalma, S., Purwanto, P., Santoso, L.W. (2015). The Effect of SO_2 and NO_2 from Transportation and Stationary Emissions Sources to SO_4^{2-} and NO_3^- in Rain Water in Semarang. *Procedia Environmental Sciences*, 23, 247–252. DOI: 10.1016/j.proenv.2015.01.037.

[12] Qu, R., Han, G. (2021). A critical review of the variation in rainwater acidity in 24 Chinese cities during 1982-2018. *Elementa*, 9(1) DOI: 10.1525/elementa.2021.00142.

[13] Goal 12: Responsible Consumption and Production - SDG Tracker. https://sdg-tracker.org/sustainable-consumption-production.

[14] Goal 15: Life on Land - SDG Tracker. https://sdg-tracker.org/biodiversity.

[15] Hagan, N. (2018). Policy assessment for the review of the primary National Ambient Air Quality Standard for sulfur oxides. In: *National Service Center for Environmental Publications*. URL: https://cfpub.epa.gov/si/si_public_record_report.cfm?Lab=OAQPS&dirEntryID=338052. Accessed 12 Oct 2023.

[16] Organization, I. M. (2020). IMO 2020 : consistent implementation of MARPOL Annex VI. In: OMi. https://www.imo.org/en/MediaCentre/HotTopics/Pages/Sulphur-2020.aspx.

[17] U.S. Energy Information Administration - EIA - Independent Statistics and Analysis. https://www.eia.gov/todayinenergy/detail.php?id=37793.

[18] Organization of Petroleum Exporting Countries. (2011). *World oil outlook*. OPEC Secretatiat.

[19] Oláh, J., Aburumman, N., Popp, J., Khan, M.A., Haddad, H., Kitukutha, N. (2020). Impact of industry 4.0 on environmental sustainability. *Sustainability (Switzerland)*, 12(11). DOI: 10.3390/su12114674.

[20] Andrienko, O., Kobotaeva, N., Skorokhodova, T., Marakina, E., Sachkov, V. (2019). A removal of sulfur-containing compounds from fuel oils using a naturally occurring iron oxyhydroxide. In: *AIP Conference Proceedings*. American Institute of Physics Inc. DOI: 10.1063/1.5099601.

[21] Wu, B., Xiong, Y., Ge, Y. (2018). Simultaneous removal of SO_2 and NO from flue gas with [rad]OH from the catalytic decomposition of gas-phase H_2O_2 over solid-phase Fe2(SO4)3. *Chemical Engineering Journal*, 331, 343–354. DOI: 10.1016/j.cej.2017.08.097.

[22] Wang, Z., Lun, L., Tan, Z., Zhang, Y., Li, Q. (2019). Simultaneous wet desulfurization and denitration by an oxidant absorbent of $NaClO_2/CaO_2$. *Environmental Science and Pollution Research*, 26(28), 29032–29040. DOI: 10.1007/s11356-019-06157-z.

[23] Li, B., Li, Y., Zhang, W., Qian, Y., Wang, Z. (2020). Simultaneous NO/SO_2 removal by coconut shell char/CaO from calcium looping in a fluidized bed reactor. *Korean Journal of Chemical Engineering*, 37(4), 688–697. DOI: 10.1007/s11814-020-0483-8.

[24] Global Sulfuric Acid Market to Surpass 324.1 Million Tons by 2027 – Coherent Market Insights | Business Wire. https://www.businesswire.com/news/home/20191122005229/en/Global-Sulfuric-Acid-Market-to-Surpass-324.1-Million-Tons-by-2027-%E2%80%93-Coherent-Market-Insights.

[25] Li, B., Ma, C. (2018). Study on the mechanism of SO_2 removal by activated carbon. *Energy Procedia*, 153, 471–477. DOI: 10.1016/j.egypro.2018.10.063.

[26] Esrafili, M.D., Heydari, S. (2018). Carbon-doped boron-nitride fullerenes as efficient metal-free catalysts for oxidation of SO_2: a DFT study. *Structural Chemistry*, 29(1), 275–283. DOI: 10.1007/s11224-017-1027-7.

[27] Esrafili, M.D. (2019). Oxidation of SO_2 over C-doped boron nitride nanosheets: The role of C-doping, and solvent effects. *Journal of Molecular Graphics and Modelling*, 86, 209–218. DOI: 10.1016/j.jmgm.2018.08.015.

[28] Jing, W., Guo, Q., Hou, Y., Han, X., Huang, Z. (2014). Study of SO_2 oxidation over V_2O_5/activated carbon catalyst using in situ diffuse reflectance infrared Fourier transformation spectroscopy. *Korean Journal of Chemical Engineering*, 31(5), 794–800. DOI: 10.1007/s11814-013-0270-x.

[29] Diez, N., Alvarez, P., Granda, M., Blanco, C., Gryglewicz, G., Wróbel-Iwaniec, I., Śliwak, A., Machnikowski, J., Menendez, R. (2014). Tailoring micro-mesoporosity in activated carbon fibers to enhance SO_2 catalytic oxidation. *Journal of Colloid and Interface Science*, 428, 36–40. DOI: 10.1016/j.jcis.2014.04.027.

[30] Mochida, I., Korai, Y., Shirahama, M., Kawano, S., Hada, T., Seo, Y., Yoshikawa, M., Yasutake, A. (2000). Removal of SOx and NOx over activated carbon fibers. *Carbon*, 38 DOI: 10.1016/S0008-6223(99)00179-7.

[31] Chiu, C.H., Kuo, T.H., Chang, T.C., Lin, S.F., Lin, H.P., Hsi, H.C. (2017). Multipollutant removal of HgO/SO_2/NO from simulated coal-combustion flue gases using metal oxide/mesoporous SiO_2 composites. *International Journal of Coal Geology*, 170, 60–68. DOI: 10.1016/j.coal.2016.08.014.

[32] Vayenas, C.G., Saltsburg, H.M. (1979). Chemistry at catalytic surfaces: The SO_2 oxidation on noble metals. *Journal of Catalysis*, 57(2), 296–314. DOI: 10.1016/0021-9517(79)90033-2.

[33] Wilburn, M.S., Epling, W.S. (2019). Formation and decomposition of sulfite and sulfate species on Pt/Pd catalysts: An SO_2 oxidation and sulfur exposure study. *ACS Catalysis*, 9(1), 640–648. DOI: 10.1021/acscatal.8b03529.

[34] Jing, W., Guo, Q., Hou, Y., Han, X., Huang, Z. (2014). Study of SO_2 oxidation over V_2O_5/activated carbon catalyst using in situ diffuse reflectance infrared Fourier transformation spectroscopy. *Korean Journal of Chemical Engineering*, 31(5), 794–800. DOI: 10.1007/s11814-013-0270-x.

[35] Qu, Z., Sun, F., Gao, J., Pi, X., Qie, Z., Zhao, G. (2019). A new insight into SO_2 lowerature catalytic oxidation in porous carbon materials: Non-dissociated O_2 molecule as oxidant. *Catalysis Science and Technology*, 9(16), 4327–4338. DOI: 10.1039/c9cy00960d.

[36] Diez, N., Alvarez, P., Granda, M., Blanco, C., Gryglewicz, G., Wróbel-Iwaniec, I., Śliwak, A., Machnikowski, J., Menendez, R. (2014). Tailoring micro-mesoporosity in activated carbon fibers to enhance SO_2 catalytic oxidation. *Journal of Colloid and Interface Science*, 428, 36–40. DOI: 10.1016/j.jcis.2014.04.027.

[37] Jing, W., Guo, Q., Hou, Y., Ma, G., Han, X., Huang, Z. (2014). Catalytic role of vanadium(V) sulfate on activated carbon for SO 2 oxidation and NH_3-SCR of NO at low temperatures. *Catalysis Communications*, 56, 23–26. DOI: 10.1016/j.catcom.2014.06.017.

[38] Guo, Q., Jing, W., Hou, Y., Li, Y., Li, F., Huang, Z. (2020). The role of vanadium species during SO_2 removal over a V_2O_5/AC catalyst. *Catalysis Science and Technology*, 10(1), 231–239. DOI: 10.1039/c9cy01975h.

[39] Chen, Y., Yin, S., Chen, Y., Cen, W., Li, J., Yin, H. (2018). Promoting mechanism of N-doped single-walled carbon nanotubes for O_2 dissociation and SO_2 oxidation. *Applied Surface Science*, 434, 382–388. DOI: 10.1016/j.apsusc.2017.10.137.

[40] Xiong, J., Li, Y., Lin, Y., Zhu, T. (2019). Formation of sulfur trioxide during the SCR of NO with NH_3 over a V_2O_5/TiO_2 catalyst. *RSC Advances*, 9(67), 38952–38961. DOI: 10.1039/c9ra08191g.

[41] Chen, Y., Yin, S., Li, Y., Cen, W., Li, J., Yin, H. (2017). Curvature dependence of single-walled carbon nanotubes for SO_2 adsorption and oxidation. *Applied Surface Science*, 404, 364–369. DOI: 10.1016/j.apsusc.2017.01.225.

[42] Yang, S., Xu, D., Yan, W., Xiong, Y. (2021). Effective NO and SO_2 removal from fuel gas with H_2O_2 catalyzed by Fe_3O_4/FeO/Fe_3C encapsulated in multi-walled carbon nanotubes. *Journal of Environmental Chemical Engineering*, 9(4). DOI: 10.1016/j.jece.2021.105413.

[43] Cen, W., Hou, M., Liu, J., Yuan, S., Liu, Y., Chu, Y. (2015). Oxidation of SO_2 and NO by epoxy groups on graphene oxides: The role of the hydroxyl group. *RSC Advances*, 5(29), 22802–22810. DOI: 10.1039/c4ra15179h.

[44] Zhang, H., Cen, W., Liu, J., Guo, J., Yin, H., Ning, P. (2015). Adsorption and oxidation of SO_2 by graphene oxides: A van der Waals density functional theory study. *Applied Surface Science*, 324, 61–67. DOI: 10.1016/j.apsusc.2014.10.087.

[45] He, G., He, H., He, H., He, H. (2020). Water Promotes the Oxidation of SO_2 by O_2 over Carbonaceous Aerosols. *Environmental Science and Technology*, 54(12), 7070–7077. DOI: 10.1021/acs.est.0c00021.

[46] Zou, L., Yan, P., Lu, P., Chen, D., Chu, W., Cen, W. (2020). Enhanced heterogenous hydration of SO_2 through immobilization of pyridinic-N on carbon materials: Hydration of SO_2 on PyN doped Carbon. *Royal Society Open Science*, 7(8) DOI: 10.1098/rsos.192248.

[47] Esrafili, M.D. (2019). Oxidation of SO_2 over C-doped boron nitride nanosheets: The role of C-doping, and solvent effects. *Journal of Molecular Graphics and Modelling*, 86, 209–218. DOI: 10.1016/j.jmgm.2018.08.015.

[48] Esrafili, M.D., Heydari, S. (2018). Carbon-doped boron-nitride fullerenes as efficient metal-free catalysts for oxidation of SO_2: a DFT study. *Structural Chemistry*, 29(1), 275–283. DOI: 10.1007/s11224-017-1027-7.

[49] Li, B., Ma, C. (2018). Study on the mechanism of SO_2 removal by activated carbon. In: *Energy Procedia*. Elsevier Ltd, pp. 471–477. DOI: 10.1016/j.egypro.2018.10.063.

[50] Du, X., Xue, J., Wang, X., Chen, Y., Ran, J., Zhang, L. (2018). Oxidation of Sulfur Dioxide over V_2O_5/TiO_2 Catalyst with Low Vanadium Loading: A Theoretical Study. *Journal of Physical Chemistry C*, 122(8), 4517–4523. DOI: 10.1021/acs.jpcc.8b00296.

[51] Dunn, J.P., Stenger, H.G.B., Wachs, I.E. (1999). Oxidation of sulfur dioxide over supported vanadia catalysts: molecular structure ± reactivity relationships and reaction kinetics. *Catalysis Today*, 51(2), 301–308. DOI: 10.1016/S0920-5861(99)00052-8.

[52] Lai, J.K., Wachs, I.E. (2018). A Perspective on the Selective Catalytic Reduction (SCR) of NO with NH_3 by Supported V_2O_5-WO_3/TiO2 Catalysts. *ACS Catalysis*, 8(7), 6537–6551. DOI: 10.1021/acscatal.8b01357.

[53] Kamata, H., Ohara, H., Takahashi, K., Yukimura, A., Seo, Y. (2001). SO_2 oxidation over the V_2O_5/TiO_2 SCR catalyst. *Catalysis Letters*, 73(1). DOI: 10.1023/A:1009065030750.

[54] Xiong, J., Li, Y., Lin, Y., Zhu, T. (2019). Formation of sulfur trioxide during the SCR of NO with NH_3 over a V_2O_5/TiO_2 catalyst. *RSC Advances*, 9(67), 38952–38961. DOI: 10.1039/c9ra08191g.

[55] N.-Y., T. (1995). Vanadia/Titania catalysts for selective catalytic reduction (SCR) of nitric oxide by ammonia. *Journal of Catalysis*, 226–240. DOI: 10.1006/jcat.1995.1024.

[56] Lai, J.K., Wachs, I.E. (2018). A perspective on the selective catalytic reduction (SCR) of NO with NH3 by supported V_2O_5-WO_3/TiO_2 catalysts. *ACS Catalysis*, 8(7), 6537–6551. DOI: 10.1021/acscatal.8b01357.

[57] He, Y., Ford, M.E., Zhu, M., Liu, Q., Wu, Z., Wachs, I.E. (2016). Selective catalytic reduction of NO by NH_3 with WO_3-TiO_2 catalysts: Influence of catalyst synthesis method. *Applied Catalysis B: Environmental*, 188, 123–133. DOI: 10.1016/j.apcatb.2016.01.072.

[58] Qing, M., Su, S., Wang, L., Liu, L., Xu, K., He, L., Jun, X., Hu, S., Wang, Y., Xiang, J. (2019). Getting insight into the oxidation of SO_2 to SO_3 over V_2O_5-WO_3/TiO_2 catalysts: Reaction mechanism and effects of NO and NH_3. *Chemical Engineering Journal*, 361, 1215–1224. DOI: 10.1016/j.cej.2018.12.165.

[59] Svachula, J., Ferlazzo, N., Tronconi, E., Bregani, F. (1993). Selective reduction of NOx by NH_3 over honeycomb DeNOxing catalysts. *Industrial and Engineering Chemistry Research*, 32, 1053–1060. DOI: 10.1021/ie00018a010.

[60] Shi, Y., Fan, M. (2007). Reaction kinetics for the catalytic oxidation of sulfur dioxide with microscale and nanoscale iron oxides. *Industrial and Engineering Chemistry Research*, 46(1), 80–86. DOI: 10.1021/ie060889d.

[61] Koutsopoulos, S., Eriksen, K.M., Fehrmann, R. (2006). Synthesis and characterization of supported Pt and Pt alloys nanoparticles used for the catalytic oxidation of sulfur dioxide. *Journal of Catalysis*, 238(2), 270–276. DOI: 10.1016/j.jcat.2005.12.009.

[62] Yan, Z., Kang, Y., Li, D., Liu, Y.C. (2020). Catalytic oxidation of sulfur dioxide over α-Fe_2O_3/SiO_2 catalyst promoted with Co and Ce oxides. *Korean Journal of Chemical Engineering*, 37(4), 623–632. DOI: 10.1007/s11814-020-0477-6.

[63] Liu, H., Zhang, Q., Yang, H., Wu, Y., Chen, J., Hu, S. (2021). Effect of metal oxides and smelting dust on SO_2 conversion to SO_3. *Atmosphere*, 12(6) DOI: 10.3390/atmos12060734.

[64] Hammerle, R.H., Truex, T.J. (1976). The Kinetics of SO_2 Oxidation for Various Catalyst Compositions.

[65] Shi, Y., Fan, M. (2007). Reaction kinetics for the catalytic oxidation of sulfur dioxide with microscale and nanoscale iron oxides. *Industrial and Engineering Chemistry Research*, 46(1), 80–86. DOI: 10.1021/ie060889d.

[66] Hamzehlouyan, T., Sampara, C., Li, J., Kumar, A., Epling, W. (2014). Experimental and kinetic study of SO_2 oxidation on a Pt/γ-Al_2O_3 catalyst. *Applied Catalysis B: Environmental*, 152–153, 108–116. DOI: 10.1016/j.apcatb.2014.01.005.

[67] Qu, Z., Sun, F., Gao, J., Pi, X., Qie, Z., Zhao, G. (2019). A new insight into SO_2 low temperature catalytic oxidation in porous carbon materials: Non-dissociated O_2 molecule as oxidant. *Catalysis Science and Technology*, 9(16), 4327–4338. DOI: 10.1039/c9cy00960d.

[68] Fixed Bed Reactor - ChemEnggHelp. https://www.chemengghelp.com/fixed-bed-reactor/#Operation_Controls_of_Fixed_Bed_Reactor.

[69] Flegkas, S., Birkelbach, F., Winter, F., Groenewold, H., Werner, A. (2019). Profitability analysis and capital cost estimation of a thermochemical energy storage system utilizing fluidized bed reactors and the reaction system MgO/$Mg(OH)_2$. *Energies*, 12(24) DOI: 10.3390/en12244788.

[70] Lappas, A., Heracleous, E. (2016). Production of biofuels via Fischer-Tropsch synthesis: Biomass-to-liquids. In: *Handbook of Biofuels Production: Processes and Technologies: Second Edition*. Elsevier Inc., pp. 549–593.DOI: 10.1016/B978-0-08-100455-5.00018-7.

[71] Thomson, C.G., Lee, A.L., Vilela, F. (2020). Heterogeneous photocatalysis in flow chemical reactors. *Beilstein Journal of Organic Chemistry*, 16, 1495–1549. DOI: 10.3762/bjoc.16.125.

[72] Ellis, N., Mahecha-Botero, A. (2020). Scale-Up of Fluidized Beds. In: Grace, J., Bi, X., Ellis, N. (eds) *Essentials of Fluidization Technology*. DOI: 10.1002/9783527699483.ch17.

[73] Sahoo, A. Studies on fluidized bed technology for treatment of gaseous pollutants: sulphur dioxide. https://www.bing.com/search?q=Studies+on+fluidized+bed+technology+for+treatment+of+gaseous+pollutants%3A+sulphur+dioxide&qs=n&form=QBRE&sp=-1&lq=1&pq=studies+on+fluidized+bed+technology+for+treatment+of+gaseous+pollutants%3A+sulphur+dioxide&sc=1-88&sk=&cvid=AA4FD4756C1343859A31038EC2DDC259&ghsh=0&ghacc=0&ghpl=. Accessed 12 Oct 2023.